SEVER INSTITUTE OF TECHNOLOGY

DOCTOR OF SCIENCE DEGREE

DISSERTATION ACCEPTANCE

(To be the first page of each copy of the dissertation)

DATE: January 28, 2004

STUDENT'S NAME: Ashoka D. Polpitiya

This student's dissertation, entitled Geometry and Control of Human Eye Movements has been examined by the undersigned committee of five faculty members and has received full approval for acceptance in partial fulfillment of the requirements for the degree Doctor of Science.

APPROVAL: _____ Chairman

_____

_____

_____

_____

WASHINGTON UNIVERSITY

SEVER INSTITUTE OF TECHNOLOGY

DEPARTMENT OF ELETRICAL AND SYSTEMS ENGINEERING

GEOMETRY AND CONTROL OF HUMAN EYE MOVEMENTS

by

Ashoka D. Polpitiya, M.S.

Prepared under the direction of Professors Bijoy K. Ghosh and W. P. Dayawansa

---

A dissertation presented to the Sever Institute of
Washington University in partial fulfillment
of the requirements for the degree of

Doctor of Science

May, 2004

Saint Louis, Missouri

WASHINGTON UNIVERSITY
SEVER INSTITUTE OF TECHNOLOGY
DEPARTMENT OF ELETRICAL AND SYSTEMS ENGINEERING

ABSTRACT

GEOMETRY AND CONTROL OF HUMAN EYE MOVEMENTS

by Ashoka D. Polpitiya

ADVISOR: Professors Bijoy K. Ghosh and W. P. Dayawansa

May, 2004
Saint Louis, Missouri

Study of human eye movements and control has been a topic among neurologists, physiologists, and engineers for a long time. In spite of several notable studies of three dimensional eye movements, there has not been a rigorous treatment of the topic in the framework of modern control theory and geometric mechanics. This thesis sheds a new light on this topic with a methodical treatment of mechanical control systems.

Attached by three pairs of muscles, the eye is treated as a rigid sphere. There is physiological evidence to support the notion that all eye movements obey Listing's law, which states that the eye orientations form a subset consisting of rotation matrices of which the axes are orthogonal to the primary gaze direction. Thus, the dynamics of the eye may be treated as a mechanical system with holonomic

constraints, which in essence limit the configuration space to be a two dimensional submanifold of $\mathsf{SO}(3)$. First we analyze the geometry of this restricted configuration space (referred to as the Listing space). As far as we are aware, this study is the first to explicitly describe the Riemannian geometry of the submanifold of Listing rotations.

Next we develop the descriptions of Lagrangian and Hamiltonian mechanics of the eye movement system in the presence of external inputs. Optimal control problems associated with the eye movement subjected to the Listing constraints will be formulated using the Maximum principle and solved numerically. The minimal distances of eye rotations with and without Listing constraints on geodesic and optimal paths are also compared.

Contents

List of Tables

List of Figures

List of Symbols

Commonly used symbols in this thesis are listed below.

Symbol	: **Description**
$\langle\ ,\ \rangle$	: metric of a Riemannian manifold
$[X, Y]$	: Lie bracket of elements X, Y of a Lie algebra
$(\mathbf{x}, \mathcal{U})$	: chart on a topological space
(θ, ϕ)	: local coordinates on ***List***
$\{\mathcal{O}_{\text{inertial}} - \boldsymbol{e}_1, \boldsymbol{e}_2, \boldsymbol{e}_3\}$	: orthonormal inertial reference frame at $\mathcal{O}_{\text{inertial}}$
$\{\mathcal{O}_{\text{body}} - \boldsymbol{b}_1, \boldsymbol{b}_2, \boldsymbol{b}_3\}$	: the orthonormal body frame fixed at $\mathcal{O}_{\text{body}}$
$\nabla_X Y$	: the Riemannian connection of Y with respect to X on a Riemannian manifold
Ψ_{*p}	: the tangent map of $\Psi : M \longrightarrow N$ between manifolds M and N at $p \in M$
$\Gamma^r(\mathsf{TM})$	: C^r-section of the tangent bundle of M
Γ_{ij}^k	: Christoffel symbols for an affine connection in a given set of coordinates
$\delta_{i,j}$	: Kronecker delta function
μ	: mass distribution
$\mu(\mathcal{B})$	: mass of a rigid body
γ	: a curve or a trajectory
$\boldsymbol{\omega}$	: body angular velocity
$\boldsymbol{\Omega}$	: 3×3 skew symmetric matrix asssociated with body angular velocity
$\boldsymbol{\xi}_c$	: center of mass
$\partial_\theta, \partial_\phi$	: short notations for $\frac{\partial}{\partial\theta}$ and $\frac{\partial}{\partial\phi}$
$\mathfrak{A}$	: Atlas on a topological space

$\mathcal{B}$	: typical rigid body
$D_X Y$	: connection or covariant derivative of Y with respect to X on a differentiable manifold M
emb	: standard map $\mathbb{R}^3 \to S^3$
$\mathfrak{F}(\mathsf{M})$	: Algebra of real-valued differentiable functions on M. i.e., $\mathfrak{F}(\mathsf{M}) = \{f : \mathsf{M} \longrightarrow \mathbb{R} \mid f \text{ is differentiable}\}$
g_{ij}	: components of the Riemannian metric $\langle\ ,\ \rangle$ also known as lower g-ij's
g^{ij}	: upper g-ij's, or (g^{ij}) is the inverse matrix of (g_{ij})
$\mathcal{H}$	: typical Hamiltonian
I	: an interval in $\mathbb{R}$
$\mathbb{I}_c$	: Inertia tensor about the center of mass
$\mathbb{I}_{\boldsymbol{\xi}_0}$	: inertia tensor about $\boldsymbol{\xi}_0$
$K(t)$	: kinetic energy
$\mathcal{J}(\Psi)(\mathbf{p})$	: Jacobian matrix of $\Psi : \mathsf{M} \to \mathsf{N}$ at $\mathbf{p}$
L	: typical Lagrangian
$\mathscr{L}_X f$	: Lie derivative of f with respect to X
List	: configuration space of the eye movement system, a submanifold of $\mathsf{SO}(3)$
$\hat{\mathbf{n}}$	: a unit vector in $\mathbb{R}^3$
$\mathbb{P}^n$	: real Projective space of dimension n
$p.q$	: quaternion product of two quaternions p and q
$p \,\mathbf{.}\, q$	: dot product of two quaternions p and q
$p^\star$	: conjugate of a quaternion p
p^{-1}	: inverse of a quaternion p
$\lvert p \rvert$	: norm of a quaternion p
$\mathbf{Q}$	: space of quaternions
Q	: configuration manifold of a mechanical system
$\mathcal{R}$	: Curvature tensor of a Riemannian manifold
$\boldsymbol{R}$	: a typical element of $\mathsf{SO}(3)$, or rotation of a rigid body about its center of mass
$\mathbb{R}$	: the set of real numbers
$\mathbb{R}^n$	: Euclidean n-space
rot	: the standard map from S^3 to $\mathsf{SO}(3)$
S^3	: unit sphere in $\mathbb{R}^4$

$\mathbf{scal}(q)$	: scalar part of the quaternion q
$\mathsf{SO}(3)$	: the space of 3×3 rotation matrices or special orthogonal group of dimension 3.
$so(3)$	: Lie algebra of the Lie group $\mathsf{SO}(3)$
$\mathsf{SU}(2)$	: special unitary group of dimension 2
$\mathsf{T}_{\mathbf{p}}\mathsf{M}$	: tangent space of a manifold M at point $\mathbf{p} \in \mathsf{M}$
TM	: the tangent bundle of a manifold M
$\mathsf{T}^\star\mathsf{M}$	: the cotangent bundle of a manifold M
$\mathbf{vec}(q)$	: vector part of the quaternion q
$\mathbf{v}_{\mathbf{p}}[f]$	: the directional derivative of f at $\mathbf{p}$ in the direction $\mathbf{v}_{\mathbf{p}}$
$\mathfrak{X}(\mathsf{M})$	: $\mathfrak{X}(\mathsf{M}) = \{X \mid X$ is a vector field on $\mathsf{M}\}$

Chapter 1

Introduction

If we knew what it was we were doing, it would not be called research, would it?

— Albert Einstein

1.1 Motivation

Biological systems are becoming more appealing to approaches that are commonly used in systems theory and suggest new design principles that may have important practical applications in man-made systems. The principles of control theory are central to many of the key questions in biological engineering.

Modeling the eye plant in order to generate various eye movements, has been the topic among neurologists, physiologists, and engineers for a long time. Since as early as 1845 (e.g. work of Listing, Donders, Helmholtz etc.), physiologists and engineers have created models in order to help understand various eye movements (see Figure 1.1) also see [Robinson 1964]. The precise coordination in muscles when the eye is rotated by the the action of 6 extra ocular muscles (EOMs), has been an important topic in treating various ocular disorders. The eyes rotate with three degrees of freedom, making it an interesting yet simpler problem compared to other complex human movement systems.

Previous studies which used modeling as a means of understanding the control of three-dimensional eye movement have adopted two main approaches. One focusing on the details of the properties of the EOMs (biomechanically "correct") [Martin & Schovanec 1998],[Miller & Robinson 1984] and the other focusing

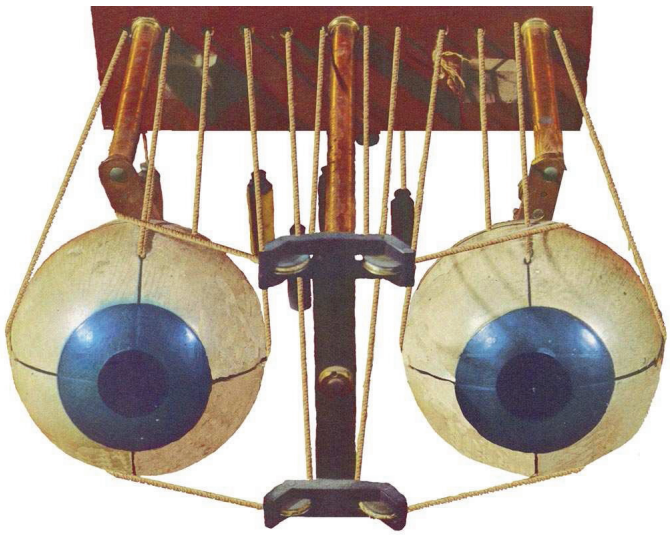

Figure 1.1: Knapp's 1861 ball and string opthalmotrop: An early mechanical model reflecting only extraocular geometry, ignoring contractile and elastic properties and coordination of inputs

on control mechanisms for three-dimensional eye movement using over simplified linear models with all the details of the above EOM properties ignored but focusing on the information processing and control aspects [Raphan 1998],[Quaia & Optican 1998].

In spite of several notable studies of three dimensional eye movements, there has not been a rigorous treatment of the topic in the framework of modern control theory and geometric mechanics. Assuming eye to be a rigid sphere, the problem can be treated as a mechanical control system which is an important and challenging research area that falls between the study of classical mechanics and modern nonlinear control. The geometric structure of mechanical systems, in general, gives way to stronger control algorithms than those obtained for generic nonlinear systems [Murray 1997].

The area of biomechanical modeling can take advantage of richly developed disciplines of mechanics and control theory. In the area of mechanics, unlike the classic approach by [Goldstein 1980], recent works by [Smale 1970*a*], [Abraham & Marsden 1987], [Krishnaprasad, Yang & Dayawansa 1991],[Marsden & Ratiu 1999], [Arnol'd 1989] and [Bullo & Lewis 2004] develop a geometric theory with Lagrangian and Hamiltonian viewpoints. Lagrangian mechanics is based on variational principles. Many important ideas in mechanics have a variational

basis [Goldstein 1980]. The Hamiltonian mechanics is directly based on the energy concept. As we see in Section 4.3, these streams are equivalent.

On the other hand control theory consists of a large as well as elegant collection of literature and specially beginning late 1970s, the works of [Brocket 1978], [Isidori 1997], and [Sussmann 1987], etc., have introduced geometric tools to nonlinear control problems. The adaptation of methods of nonlinear control theory to mechanical systems as well as extending the methods of geometric mechanics to systems with external inputs has been discussed in [Abraham & Marsden 1987], [Marsden & Ratiu 1999], [Lewis 1995] and [Bullo & Lewis 2004].

1.2 Contributions and Overview of the Thesis

The work of this dissertation may be viewed as an attempt to study and model the eye movement system as a *"simple* [1] *mechanical control system"* [Smale 1970*a*, Smale 1970*b*, Lewis & Murray 1997]. This also falls under the category of *biomechanical models*.

Attached by three pairs of muscles, the eye is treated as a rigid sphere. There is physiological evidence to support the notion that all eye movements obey Listing's law, which states that the eye orientations form a subset consisting of rotation matrices of which the axes are orthogonal to the normal (primary) gaze direction. Thus, the the eye is treated as a mechanical system with holonomic constraints, which in essence limit the configuration manifold Q to be a two dimensional submanifold of $\mathsf{SO}(3)$. This configuration manifold Q we denote as ***List***.

First we discuss in detail the geometry of ***List***. To the best of our knowledge, this study is the first to explicitly describe the Riemannian geometry of the submanifold of Listing rotations. Then the system is studied as a *forced simple mechanical system* [Bullo & Lewis 2004] with the Lagrangian formed by kinetic energy (determined by the associated Riemannian metric) minus potential energy.

Next we investigate the problem of minimizing the energy of the control. Here we follow the work by [Sussman & Willems 1997] towards the celebrated Pontryagin maximum principle in optimal control theory.

A breif outline of the content chapter-by-chapter is as follows:

[1] The word simple does not mean easy, but rather because they are not completely general. Most of the systems one encounters in applications are in fact simple mechanical systems.

Chapter 2: This chapter introduces the reader to the anatomy and structure of the human eye influencing its motion. A brief review of different modeling and control attempts is given. Chapter ends with the introduction of the famous *Listing's law*.

Chapter 3: Here we review the necessary mathematical preliminaries from differential geometry, Riemannian geometry and quaternions representing rotations.

Chapter 4: The aim of this chapter is to discuss the geometric treatment of mechanical control systems. The Lagrangian and Hamiltonian frameworks are the two main points of view. We also state the results from optimal control theory.

Chapter 5: Before the discussion of more involved topic of three-dimensional eye movements, this chapter introduces the long discussed topic of planer eye movements. A simple model with a single muscle pair to generate horizontal saccadic eye movements is discussed and a scheme to obtain the parameters of the neural control signal is proposed.

Chapter 6: In this chapter we present one of the main results of the dissertation. Geometry of the configuration space ***List*** is discussed here.

Chapter 7: Here we develop some optimal control methods on ***List***.

Chapter 8: This chapter presents some conclusions, a summary and some directions for future research.

Appendix A: In this appendix, some useful results in quaternion calculations are given.

Appendix B: This is an introduction to a muscle and a tendon complex known as "Hill-type" model. We make use of this model, in the eye movement system, as extraocular muscles.

Chapter 2

Anatomy of the Eye

Our nature consists in movement; absolute rest is death.

— Blaise Pascal (1623-1662)

Understanding how our movements are planned, controlled, and executed is a daunting task. The understanding of movements has to be based upon an accurate description of the kinematics and dynamics of the executed movements. Of all types of movements, eye movements are arguably the most appealing ones to scientific investigation. The eye is an object with negligible inertia, and only three pairs of *extraocular muscles* (EOMs) control its orientation and movement. By comparison, 24 muscles and tendons have to be taken into consideration for a 2-dimensional simplification of human walking! This large number of limb muscles is necessary for two reasons. One reason is the degrees of freedom (DOF) of limb movements: while the eye essentially displays a *ball* and *socket* behavior, and is thus restricted to only 3 DOF, leg- or arm-movements have significantly more DOFs. The other reason for the abundance of muscles in legs and arms is the inertia of limbs. While the inertia of the human eyeball is a negligible quantity [Minor, Lasker, Backous & Hullar 1999], considerable forces are necessary to accelerate or stop a limb.

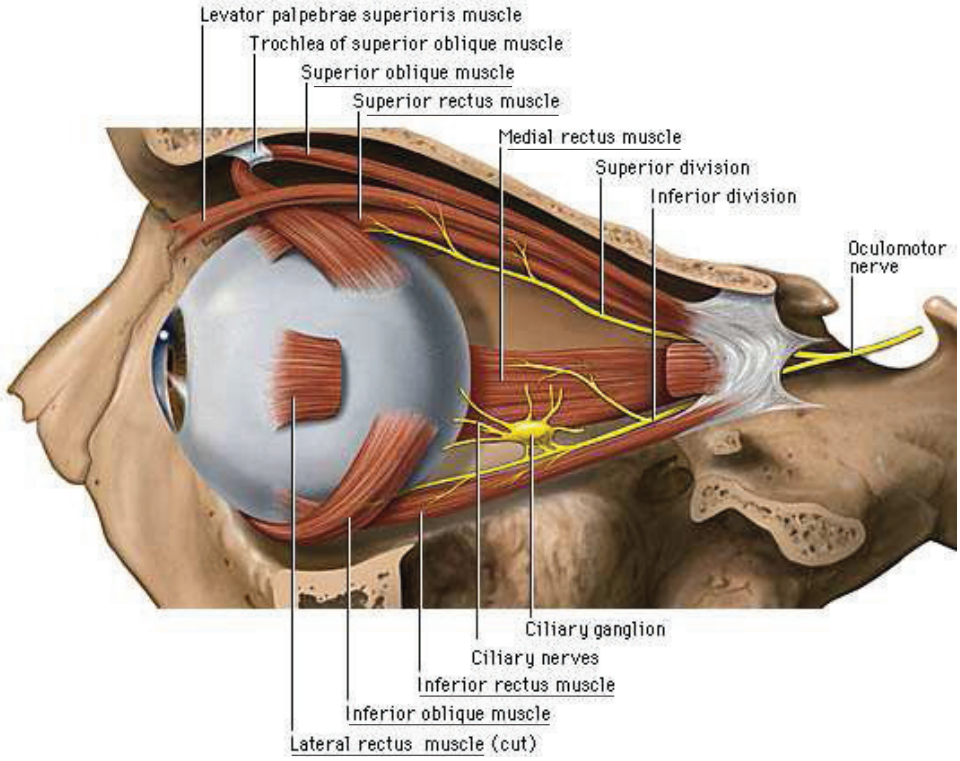

Figure 2.1: Anatomy of the eye - extraocular muscles contributing to the movement are underlined. (courtesy of Yale University School of Medicine)

2.1 Anatomy of the extraocular plant

The structures of the human eye most relevant for this study are the ones influencing or contributing to its motion. The movement of the eye is determined by the coordinated activity of the six extraocular muscles (see Figure 2.1), as well as by the mechanical properties of the tissue connecting these structures to the orbit.

The individual movements of a single eye are known as *ductions*. For example, *infraduction* (looking down), *abduction* (looking laterally or outward), *adduction* (looking medially or inward toward the nose). When both eyes function together the movements are *binocular* and termed versions of above. Each eye is moved by six extraocular muscles: ***medial*** and ***lateral rectus***, ***superior*** and ***inferior rectus***, and ***inferior*** and ***superior oblique*** muscles as shown underlined in Figure 2.1. As a first approximation they may be thought of as functioning in reciprocal pairs. For planer lateral movements of an eye, the lateral rectus contracts and the medial rectus relaxes; for planer upward movements the superior rectus contracts and inferior rectus relaxes. Diagonal and torsional movements of an

individual eye are produced by particular patterns of innervation and inhibition involving all the muscles. The main muscle producing a individual movement is known as the ***agonist***. The muscle which is simultaneously inhibited is the ***antagonist***. For example, rightward movement of the eye would result when the right lateral rectus is contracting (agonist) and the right medial rectus relaxing (antagonist). Unlike most other striated muscles which are electrically silent at rest, the extraocular muscles maintain a constant state of activity to hold the eyes in position in the orbit. The firing rate of the motorneurons supplying the extraocular musculature is controlled by higher brain and brain stem regions, the *supranuclear ocular motor control systems*.

One of the unknown factors is the exact path that the extraocular muscles take in the orbit. Recent work based on high resolution MRI scans and on transsections of the extraocular plant has revealed that the muscles do not run freely in the orbital globe. Instead, they are connected by collagen tissue and smooth muscles, sometimes referred to as *muscle pullies*, to the inner wall of the orbita [Demer, Miller, Poukens, Vinters & Glasgow 1995].

These attachments of the extraocular muscles have two important implications. First, they determine the pulling directions of the EOMs. Second, the pulling directions also play an important role for the control of eye movements. The implications of these muscle pullies for the control of eye movements are still unclear. One school of thought claims that these pullies allow the *central nervous system* (CNS) to focus on the control of the *gaze direction*, i.e., the line of sight, and leave the adjustment of the eye orientation (or the *torsion* about the gaze direction) to the mechanics of the eye plant [Raphan 1998]. In fact, recordings of the activity of single neurons in the *superior colliculus*, a midbrain structure that is very important for the generation of fast eye movements, have shown that at that stage the signal that controls the eye movement is represented only in 2-dimensions [van Opstal, Hepp, Hess, Straumann & Henn 1991]. The other school of thought insists that the eye movement is controlled in all three directions, taking into consideration the effects of the EOMs [Tweed, Haslwanter & Fetter 1998]. In their opinion the system accurately controls and executes movements of the eyes, also accounting for the torsion. While the first model requires 2 degrees of freedom for eye movement control, the second model implies a fully 3-dimensional control structure on $\mathsf{SO}(3)$. We will mention a word or two on this two schools of thinking

again in section 2.3 when we discuss about the Listing's law and it will become clearer afterwards.

2.2 Movements of the eye

There are four separate subsystems of supranuclear ocular motor control, each with different neurophysiologic characteristics and largely separate neuroanatomic pathways. The four subsystems are: (1) ***Saccadic*** or fast eye movement subsystems, (2) ***Pursuit*** or tracking subsystem, (3)***Vestibular Ocular Reflex (VOR)*** subsystem, and (4) ***Vergence*** subsystem.

The two main tasks of the eye are reflected in its movements: the eye has to be able to generate a stable image on the retina, and to shift the point of interest quickly to a new target. In primates, the fovea (the central part of retina where the optimal visual resolution is achieved) has an effective diameter of less than a degree. Therefore, whenever the primate visual system decides to further explore the details of a peripheral visual target, the current gaze line must be precisely redirected at the object. Such fast eye movements necessary for target shifts are called ***saccades***. Saccades are only used to change the gaze direction, and no visual information is obtained during the saccadic gaze shift. The sudden appearance of a peripheral object or an eccentric sound may evoke a reflex saccade in the direction of the stimulus, typically with a latency of 200 to 250 msec. In humans they reach velocities ranging from $30^0/s$ to $700^0/s$, for movements from 0.5 degrees to 40 degrees in amplitude, and are executed in a very stereotyped way. Saccades are ballistic (i.e., happens under open-loop control, and cannot be altered once the motion is initiated). The control signal is the retinal position error. Apart from astonishingly fast, often lasting little more than 20 milliseconds, they also happen to be the single most frequent movement we make, much commoner than heartbeats; we make two or three saccades every second of our waking lives.

While saccades that are executed with the head stationary are well understood, combined eye-head movements have only recently become the focus of research. Once the eye has reached its target, the CNS has to ensure that the visual information is clear and does not get blurred by voluntary or involuntary head movements. This is achieved by the *pursuit eye movements* and *vestibulo-ocular reflex (VOR)*. The major stimulus for a pursuit eye movement is a slow movement

of a fixated target. This evokes a following eye movement after latency of 125 msec. The maximum pursuit velocities can go upto $50^0/s$. The input signal is the retinal error ("slip") velocity. It may be interesting to note here that it is not possible to generate smooth pursuit eye movements without an actual smoothly moving target. Attempts to voluntarily move the eyes smoothly without actual target motion result in a series of small saccades, so called "cog-wheel" pursuit.

The VOR movement compensates for the movement of the head, thereby ensuring a clear image of the fixation object on the retina. The latency can be up to 100 msec and the peak eye velocity can be in the order of $300^0/s$. VOR takes place as a smooth movement under continous feedback control with possible interruptions by intermittent saccades which recenter the eyes toward a midposition in the orbit. This repetitive pattern of slow and fast eye movements is an example of one type of nystagmus. Nystagmus is an ocular oscillation with repetitive to and from movements, usually composed of a slow component and a fast or saccadic component.

The stimuli for the fourth type, the vergence eye movements are target displacement or motion along the gaze axis (toward or away from the observer). The latency for vergence eye movements is approximately 160 msec; maximum velocities are in the range of $20^0/s$, and the system is unique in being able to generate uniocular eye movements. For example, if a target were placed exactly in front of the right eye and slowly brought closer to the observer, the right eye would remain stationary but the left eye would converge.

2.3 Listing's law

Eye Positions. In what follows, a 3 dimensional eye position is parametrized by the *virtual* rotation that brings the eye from the primary position (usually taken as the straight ahead gaze direction) to the current position. A *secondary* eye position is obtained by a rotation from the primary position about either the horizontal or vertical axis of the primary coordinate system. A *tertiary* position is any position that obeys Listing's law (see below) and is not a primary or secondary position.

Donder's law. While looking at a target, the position of the target determines the gaze direction, but does not specify the orientation (or the amount of "torsion"-as

often referred in ocular physiology- about the gaze line). Donders in 1848 discovered that this amount of torsion is not arbitrary, but uniquely determined by the gaze direction and independent of the trajectory followed to get to that position. In other words, ocular torsion is fully specified by the horizontal and vertical components of the gaze direction, i.e., a two-dimensional subspace. This phenomena is known as *Donder's law* . The precise geometry of this subspace however, is not specified by Donder's law.

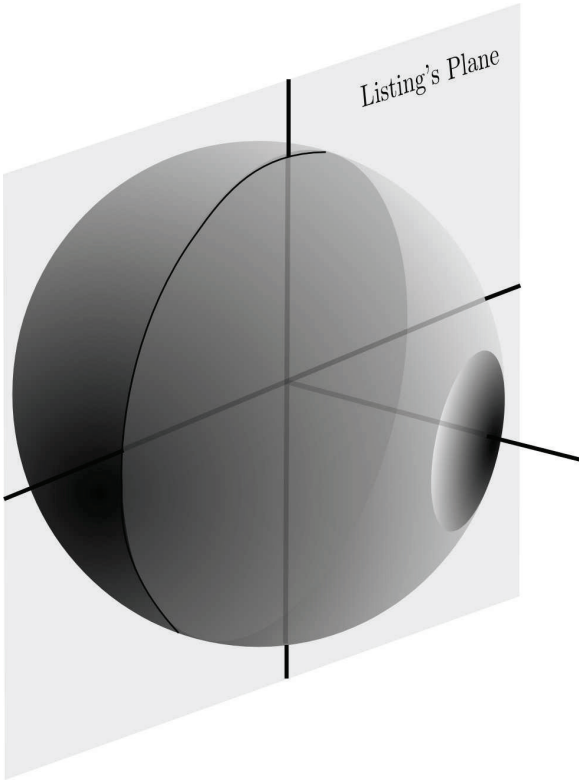

Figure 2.2: Listing's plane

Listing's law. By following a suggestion by the German physicist Listing, Helmholtz further investigated this idea and was able to specify this amount. He proposed that the Donder's surface is in fact a plane. This is known as the *Listing's plane* and the phenomena is called the *Listing's law*. Stated loosely, Listing's law says all eye positions can be reached from the so called *primary position* by picking up axes of rotations scattered along a plane. But let's state it in a more 'mathematical language'.

Listing's law: All rotation matrices employed to direct the gaze vector from the primary position to a tertiary position have their axes of rotations orthogonal to the primary gaze direction. This in turn resolves the ambiguity of specifying the orientation (torsion) while looking at a target by restricting the natural configuration space $\mathsf{SO}(3)$ of the eye movements to a submanifold of $\mathsf{SO}(3)$.

How the eye obeys Listing's law is still not clear. The debate between the two schools of thought mentioned in Section 2.1 boils down to the question of whether the structure of the eye plant with pullies in fact satisfies the Listing's law or is it the CNS which generates the necessary motor commands to move the eye following the Listing's criterion. In this thesis we align with the later since their is not enough evidence in the structure of the eye to support the former though there have been arguments that the newly discovered pullies may play a role [Demer, Oh & Poukens 2000], [Raphan 1998], and [Quaia & Optican 1998].

Chapter 3

Mathematical Preliminaries

Let no one enter who does not know geometry.

— Inscription on Plato's door

The treatment of eye movement problem in this thesis is geometric. Therefore, to collect the necessary mathematical tools, a list of definitions and theorems from differential geometry is given first in this chapter. From the general concepts of differential geometry the focus quickly moves, in Section 3.2, to Riemannian geometry (Riemannian metrics, Riemannian connections, geodesics and curvature). For a thorough treatment of the basic differential and Riemannian geometric ideas, one should refer the texts [Boothby 1986], [do Carmo 1993] and [Warner 1989]. In Section 3.3, a discussion on Quaternions to represent rotations in $\mathbb{R}^3$ is given. Again, one should refer to texts by [Kuipers 1998] and [Conway & Smith 2003] for a detailed account.

3.1 Differential Geometry

The basic object in differential geometry is the *manifold*, which generally speaking, is a topological space resembling to an open subset of Euclidean space locally. A *differentiable manifold* is a manifold M for which this resemblance is sharp enough to allow partial differentiation and consequently all the features of differential calculus on M. Let's make precise the "local resemblance".

3.1.1 Differentiable Manifolds and maps

Charts and Atleses

Definition 3.1. *A* **chart** *on a topological space* M *is a pair* $(\mathbf{x}, \mathcal{U})$*, where* $\mathcal{U}$ *is an open subset of* $\mathbb{R}^n$ *and*

$$\mathbf{x} : \mathcal{U} \longrightarrow \mathbf{x}(\mathcal{U}) \subset \mathsf{M}$$

is a homeomorphism[1] *of* $\mathcal{U}$ *onto an open set* $\mathbf{x}(\mathcal{U})$ *of* M*. Here* $\mathbf{x}$ *is called the* **local homeomorphism** *of the chart, and* $\mathbf{x}(\mathcal{U})$ *the* **coordinate neighborhood.** *Frequently, we refer to "the chart* $\mathbf{x}$*" when the domain* $\mathcal{U}$ *is understood. Let*

$$x_i = u_i \circ \mathbf{x}^{-1} : \mathbf{x}(\mathcal{U}) \longrightarrow \mathbb{R}$$

for $i = 1, \ldots, n$*. Then* x_i *is called the* i^{th}**-coordinate function**, *and* $(x_1, \ldots, x_n)$ *is called a* **system of local coordinates** *for* M*.*

Following the same procedure as in the case of collection of geographical maps or **charts** that covers the earth is called an **atlas**, one can arrive the definition of the differentiable manifold.

Definition 3.2. *An* **atlas** $\mathfrak{A}$ *on a topological space* M *is a collection of charts on* M *such that all the charts map from open subsets of the same Euclidean space* $\mathbb{R}^n$ *into* M*, and* M *is the union of all the* $\mathbf{x}(\mathcal{U})$*'s such that* $(\mathbf{x}, \mathcal{U}) \in \mathfrak{A}$*. A topological space* M *equipped with an atlas is called a* **topological manifold**.

Change of coordinates. Let $\mathfrak{A}$ be an atlas on a topological space M. Notice that if $(\mathbf{x}, \mathcal{U})$ and $(\mathbf{y}, \mathcal{V})$ are two charts in $\mathfrak{A}$ such that $\mathbf{x}(\mathcal{U}) \cap \mathbf{y}(\mathcal{V}) = \mathcal{W} \subset \mathsf{M}$ is nonempty, then the map

$$(\mathbf{x}^{-1} \circ \mathbf{y}) : \mathbf{y}^{-1}(\mathcal{W}) \longrightarrow \mathbf{x}^{-1}(\mathcal{W}) \tag{3.1}$$

is a homeomorphism between open subsets of $\mathbb{R}^n$. We call $(\mathbf{x}^{-1} \circ \mathbf{y})$ a **change of coordinates**.

Definition 3.3. *A* **differentiable manifold** *is a paracompact*[2] *Hausdorff*[3] *topological space* M *equipped with an atlas* $\mathfrak{A}$ *such that for any two charts* $(\mathbf{x}, \mathcal{U}), (\mathbf{y}, \mathcal{V}) \in \mathfrak{A}$ *with*

[1] One-to-one correspondence between points in two topological spaces which is continuous in both directions, also called a continuous transformation.

[2] A paracompact space is a Hausdorff space such that every open cover has a locally finite open refinement.

[3] stated loosely, ...any two points have disjoint neighborhoods.

$\mathbf{x}(\mathcal{U}) \cap \mathbf{y}(\mathcal{V}) = \mathcal{W}$ *nonempty, the change of coordinates (3.1) is differentiable (i.e. of class* C^∞*) in the ordinary Euclidean sense. The* **dimension** *of the manifold* M *(denoted by* $dim\mathsf{M}$*) is the dimension of* $\mathcal{U}$ *for any* $(\mathbf{x}, \mathcal{U}) \in \mathfrak{U}$.

Differentiable functions on differentiable manifolds

Definition 3.4. *Let* $f : \mathcal{W} \subset \mathsf{M} \longrightarrow \mathbb{R}$ *be a function defined on an open subset* $\mathcal{W}$ *of a differentiable manifold* M*. We say that* f *is* **differentiable** *at* $\mathbf{p} \in \mathcal{W}$*, provided that for some chart* $\mathbf{x} : \mathcal{U} \subset \mathbb{R}^n \longrightarrow \mathsf{M}$ *with* $\mathbf{p} \in \mathbf{x}(\mathcal{U}) \subset \mathcal{W}$*, the composition* $f \circ \mathbf{x} : \mathcal{U} \subset \mathbb{R}^n \longrightarrow \mathbb{R}$ *is differentiable at* $\mathbf{x}^{-1}(\mathbf{p})$*. If* f *is differentiable at all points of* $\mathcal{W}$*, we say that* f *is* **differentiable** *on* $\mathcal{W}$.

It is a direct consequence using the change of coordinates, that the above differentiability is independent of the choice of the chart.
We denote

$$\mathfrak{F}(\mathsf{M}) = \{f : \mathsf{M} \to \mathbb{R} |\ f \text{ is differentiable}\}.$$

$\mathfrak{F}(\mathsf{M})$ is called the **algebra of real-valued differentiable functions** on M.

Maps between manifolds

With the notion of real-valued differentiable functions on a differentiable manifold, one can define the differentiable maps between manifolds.

Definition 3.5. *let* M *and* N *be differentiable manifolds, and let* $\Psi : \mathsf{M} \longrightarrow \mathsf{N}$ *be a map. We say that* Ψ *is* **differentiable**, *provided that* $\mathbf{y}^{-1} \circ \Psi \circ \mathbf{x}$ *is differentiable for every chart* $(\mathbf{x}, \mathcal{U})$ *in the atlas of* M *and every chart* $(\mathbf{y}, \mathcal{V})$ *in the atlas of* N*, where the compositions are defined. A* **diffeomorphism** *between manifolds* M *and* N *is a differentiable map* $\Phi : \mathsf{M} \longrightarrow \mathsf{N}$ *which has a differentiable inverse* $\Phi^{-1} : \mathsf{N} \longrightarrow \mathsf{M}$*. If such a map* Ψ *exists,* M *and* N *are said to be* **diffeomorphic**.

It is an easy consequence that the composition of two differentiable maps is again differentiable.

3.1.2 Tangent bundle and Induced maps

In Lagrangian mechanics, tangent bundle, which is a manifold itself, is the state space of the system. Therefore, it plays a crucial role in our study. In mechanics,

tangent bundle can be thought of as the set of positions and velocities when the positions of the system is treated as a manifold. It is an interesting fact to see that one can only speak of velocities at a given *position*. This section defines the velocities, i.e., tangent vectors at a given point on the manifold.

Tangent vectors

Definition 3.6 (Tangent vector). *Let* $\mathbf{p}$ *be a point of a manifold* M*. A* **tangent vector** $\mathbf{v}_\mathbf{p}$ *to* M *at* $\mathbf{p}$ *is a real-valued function* $\mathbf{v}_\mathbf{p} : \mathfrak{F}(\mathsf{M}) \longrightarrow \mathbb{R}$ *such that*

$$\begin{aligned} \mathbf{v}_\mathbf{p}[af + bg] &= a\mathbf{v}_\mathbf{p}[f] + b\mathbf{v}_\mathbf{p}[g] && \text{(the } \textbf{linearity} \text{ property)}, \\ \mathbf{v}_\mathbf{p}[fg] &= f(\mathbf{p})\mathbf{v}_\mathbf{p}[g] + g(\mathbf{p})\mathbf{v}_\mathbf{p}[f] && \text{(the } \textbf{Leibnizian} \text{ property)}, \end{aligned}$$

for all $a, b \in \mathbb{R}$ *and* $f, g \in \mathfrak{F}(\mathsf{M})$*.*

Roughly speaking, $\mathbf{v}_\mathbf{p}[f]$ is the ordinary derivative of f at $\mathbf{p}$ along a curve leaving $\mathbf{p}$ in the direction $\mathbf{v}_\mathbf{p}$.

From these properties it is clear that for a chart $(\mathbf{x}, \mathcal{U})$ on a differentiable manifold M and for a $\mathbf{p} \in \mathbf{x}(\mathcal{U})$, the function

$$\left.\frac{\partial}{\partial x_i}\right|_\mathbf{p} p : \mathfrak{F}(\mathsf{M}) \longrightarrow \mathbb{R}$$

defined by

$$\left.\frac{\partial}{\partial x_i}\right|_\mathbf{p} [f] = \left.\frac{\partial f}{\partial x_i}\right|_\mathbf{p}$$

is a tangent vector to M at $\mathbf{p}$ for $i = 1, \ldots, n$.

Definition 3.7 (Tangent bundle). *The* **tangent space** *to a differentiable manifold* M *at point* $\mathbf{p} \in \mathsf{M}$ *is the set of all tangent vectors to* M *at* $\mathbf{p}$ *and is denoted by* $\mathsf{T}_\mathbf{p}\mathsf{M}$*. The collection*

$$\mathsf{TM} = \bigcup_{\mathbf{p} \in \mathsf{M}} \mathsf{T}_\mathbf{p}\mathsf{M}$$

of all tangent spaces is called the **tangent bundle***. The* **tangent bundle projection** *map* $\pi_{\mathsf{TM}} : \mathsf{TM} \to \mathsf{M}$ *by* $\pi_{\mathsf{TM}}(v) = \mathbf{p}$ *when* $v \in \mathsf{T}_\mathbf{p}\mathsf{M}$*.*

It can be proved that $\mathsf{T}_{\mathbf{p}}\mathsf{M}$ is indeed a finite-dimensional vector space whose dimension is the same as that of M. The natural candidate for the basis of $\mathsf{T}_{\mathbf{p}}\mathsf{M}$ is

$$\left\{ \left.\frac{\partial}{\partial x_1}\right|_{\mathbf{p}}, \ldots, \left.\frac{\partial}{\partial x_n}\right|_{\mathbf{p}} \right\}.$$

Therefore one can write $\mathbf{v}_{\mathbf{p}} \in \mathsf{T}_{\mathbf{p}}\mathsf{M}$ as

$$\mathbf{v}_{\mathbf{p}} = \sum_{i=1}^{n} \mathbf{v}_{\mathbf{p}}[x_i] \left.\frac{\partial}{\partial x_i}\right|_{\mathbf{p}}. \tag{3.2}$$

where $x_1, \ldots, x_n$ are coordinate functions, i.e. $\mathbf{x}^{-1} = (x_1, \ldots, x_n)$.
The **cotangent space** $\mathsf{T}^{\star}_{\mathbf{p}}\mathsf{M}$ is the dual space to $\mathsf{T}_{\mathbf{p}}\mathsf{M}$, i.e., the set of linear functionals on $\mathsf{T}_{\mathbf{p}}\mathsf{M}$. In a similar fashion one can define the **cotangent bundle** $\mathsf{T}^{\star}\mathsf{M}$.

Induced maps

Definition 3.8. *Let $\Psi : \mathsf{M} \to \mathsf{N}$ be a differentiable map between differentiable manifolds M and N, and let $\mathbf{p} \in \mathsf{M}$. Then the* **tangent map** *of Ψ at $\mathbf{p}$ is the map*

$$\Psi_{\star\mathbf{p}} : \mathsf{T}_{\mathbf{p}}\mathsf{M} \to \mathsf{T}_{\Psi(\mathbf{p})}\mathsf{N}$$

given by

$$\Psi_{\star\mathbf{p}}(\mathbf{p})[f] = \mathbf{v}_{\mathbf{p}}[f \circ \Psi]$$

for each $f \in \mathfrak{F}(\mathsf{N})$ and $\mathbf{v}_{\mathbf{p}} \in \mathsf{T}_{\mathbf{p}}\mathsf{M}$.

Definition 3.9 (Jacobian matrix). *Let $\Psi : \mathsf{M} \to \mathsf{N}$ be a differentiable map, where M is an m-dimensional manifold and N is an n-dimensional manifold. Let $\mathbf{p} \in \mathsf{M}$, $(\mathbf{x}, \mathcal{U})$ a chart on M at $\mathbf{p}$ and $(\mathbf{y}, \mathcal{V})$ a chart on N at $\Psi(\mathbf{p})$. The* **Jacobian matrix** *$\mathcal{J}(\Psi)(\mathbf{p})$ of Ψ at $\mathbf{p}$ relative to $\mathbf{x}$ and $\mathbf{y}$ is the matrix of $\Psi_{\star\mathbf{p}}$ relative to the bases*

$$\left\{ \left.\frac{\partial}{\partial x_1}\right|_{\mathbf{p}}, \ldots, \left.\frac{\partial}{\partial x_m}\right|_{\mathbf{p}} \right\} \quad \text{and} \quad \left\{ \left.\frac{\partial}{\partial y_1}\right|_{\Psi(\mathbf{p})}, \ldots, \left.\frac{\partial}{\partial y_n}\right|_{\Psi(\mathbf{p})} \right\}.$$

Explicitly, $\mathcal{J}(\Psi)(\mathbf{p})$ is the matrix

$$\left(\frac{\partial(y_j \circ \Psi)}{\partial x_i}(\mathbf{p}) \right).$$

With the concepts developed so far one can discuss the notion of a *curve* on a manifold. Let I denotes an open interval of the real line $\mathbb{R}$, and d/du the natural coordinate vector field on it. For each $t \in I$ we have a canonical tangent vector in $\mathsf{T}_t\mathbb{R}$, as

$$\left.\frac{d}{dt}\right|_t.$$

Definition 3.10. *A* **curve** *on a differentiable manifold* M *is a differentiable function* $\boldsymbol{\alpha} : I \to \mathsf{M}$*. If* $t \in I$*, the* **velocity vector** *of* $\boldsymbol{\alpha}$ *at* t *is the tangent vector*

$$\boldsymbol{\alpha}'(t) = \boldsymbol{\alpha}_{\star t}\left(\left.\frac{d}{du}\right|_t\right) \in \mathsf{T}_{\boldsymbol{\alpha}(t)}\mathsf{M}.$$

The value of the velocity vector $\boldsymbol{\alpha}'(t)$ on a function $f \in \mathfrak{F}(\mathsf{M})$ is given by

$$\boldsymbol{\alpha}'(t)[f] = \frac{d(f \circ \boldsymbol{\alpha})}{du}(t).$$

It is an immediate consequence from Equation (3.2) to write this as

$$\boldsymbol{\alpha}'(t)[f] = \sum_{i=1} n \frac{d(x_i \circ \boldsymbol{\alpha})}{du}(t) \left.\frac{\partial}{\partial x_i}\right|_{\boldsymbol{\alpha}(t)}.$$

3.1.3 Vector and Tensor fields on manifolds

A **vector field** X on a differentiable manifold M is a correspondence that associates to each point $\mathbf{p} \in \mathsf{M}$ a vector $X_\mathbf{p} \in \mathsf{T}_\mathbf{p}\mathsf{M}$. In terms of mappings, X is a mapping of M into the tangent bundle TM. The field is **differentiable** if the mapping $X : \mathsf{M} \to \mathsf{TM}$ is differentiable.

Similarly, a **one-form** ω on M associates to each $\mathbf{p} \in \mathsf{M}$ a cotangent vector $\omega_\mathbf{p}$. Finally, a **tensor** α of covariant order r and contravariant order s associates to each $\mathbf{p} \in \mathsf{M}$ a multi-linear map $\alpha : \mathsf{TM} \times \ldots \mathsf{TM} \times \mathsf{T}^\star\mathsf{M} \times \ldots \times \mathsf{T}^\star\mathsf{M} \to \mathbb{R}$ (with r copies of TM and s copies of $\mathsf{T}^\star\mathsf{M}$).
We denote

$$\mathfrak{X} = \{X | X \text{ is a vector field on } \mathsf{M}\}.$$

A **covariant tensor field of degree** r on a differentiable manifold M is a mapping

$$\alpha : \mathfrak{X}(\mathsf{M}) \times \cdots \times \mathfrak{X}(\mathsf{M}) \to \mathfrak{F}(\mathsf{M})$$

that satisfies

$$\begin{aligned}\alpha(X_1,\ldots,f_iY_i+g_iZ_i,\ldots,X_r) &= f_i\alpha(X_1,\ldots,Y_i,\ldots,X_r)\\ &\quad +g_i\alpha(X_1,\ldots,Z_i,\ldots,X_r)\end{aligned}\tag{3.3}$$

for all $f_i, g_i \in \mathfrak{F}(\mathsf{M})$, $X_1,\ldots,X_r, Y_i, Z_i \in \mathfrak{X}(\mathsf{M})$. A **vectorvariant tensor field** is a mapping

$$\Phi : \mathfrak{X}(\mathsf{M}) \times \cdots \times \mathfrak{X}(\mathsf{M}) \to \mathfrak{X}(\mathsf{M})$$

that satisfies (3.3).

Examples 3.1.1: 1. A **vector field** is a $(1,0)$-tensor field on M.

2. A **covector field** is a $(0,1)$-tensor field on M.

3. A **Riemannian metric** on M is a $(0,2)$-tensor field g on M (see Section 3.2).

Associated with each vector field $X \in \mathfrak{X}(\mathsf{M})$ is a **section** of TM, that is, a differentiable map $X : \mathsf{M} \to \mathsf{TM}$ such that $\pi \circ X = id_{\mathsf{M}}$, where id_{M} denotes the identity map on M. In particular, X is a map that associates a tangent vector $X_{\mathbf{p}} \in \mathsf{T}_{\mathbf{p}}\mathsf{M}$ with each point $\mathbf{p} \in \mathsf{M}$. Conversely, each section of the tangent bundle gives rise in a natural way to an element of $\mathfrak{X}(\mathsf{M})$.

Vector fields and differential equations have some relationships in common: a tangent vector to a curve $\gamma : I \to \mathsf{M}$ is equal to the tangent vector specified by the vector field at each point along the curve. In a coordinate chart, to determine integral curves one obtains the solution of a differential equation.

A vector field along a curve $\boldsymbol{\gamma} : (a,b) \to \mathsf{M}$ is a function $\mathbf{Y}$ that assigns to each t with $a < t < b$ a tangent vector $\mathbf{Y}(t) \in \mathsf{M}_{\gamma(t)}$.

Given a function $f \in \mathfrak{F}(\mathsf{M})$ we let $\mathscr{L}_X f$ denote the **Lie derivative** of f with respect to X (sometimes written as $X[f]$) and we let $\mathrm{d}f$ denote the one-form such that for all vector fields X:

$$\langle \mathrm{d}f, X\rangle = \mathscr{L}_X f$$

where $\langle\cdot,\cdot\rangle$ denote the standard pairing between tangent and cotangent spaces.

Given a pair of smooth vector fields X, Y, we let $[X,Y]$ denote their Lie bracket and let $\mathscr{L}_X Y$ denote the Lie derivative of Y with respect to X (sometimes written as just XY).

Definition 3.11 (Lie bracket). *For $X, Y \in \mathfrak{X}(\mathsf{M})$ the vector field $[X, Y]$ defined by*

$$\mathscr{L}_{[X,Y]} f = \mathscr{L}_X \mathscr{L}_Y f - \mathscr{L}_Y \mathscr{L}_X f, \qquad f \in \mathfrak{F}(\mathsf{M}),$$

is the **Lie bracket** *of X and Y, or the* **Lie derivative** *of Y with respect to X.*

Sometimes, the notations, $\mathrm{ad}_X Y = [X, Y]$ and $\mathscr{L}_X Y = [X, Y]$ are used by some authors.

Lie bracket satisfies two fundamental properties: skew symmetry and the Jacobi identity:

$$[[X, Y], Z] + [[Y, Z], X] + [[Z, X], Y] = 0.$$

In nonlinear control theory, Lie bracket $[X, Y]$ is usually interpreted as a derivation of Y along the *trajectories* of X. In particular, if we flow along X, then Y, then $-X$, then $-Y$, all with the same time, and if we return to the same point, then $[X, Y](x) = 0$ for $x \in \mathsf{M}$. Then the vector fields X and Y are said to **commute**.

3.1.4 Affine connections

For a general differentiable manifold, there is no natural notion of differentiation of vector fields. Hence the following definition.

Definition 3.12. *An* **affine connection** *or* **covariant derivative** *on a differentiable manifold* M *is a map*

$$\nabla : \mathfrak{X}(\mathsf{M}) \times \mathfrak{X}(\mathsf{M}) \to \mathfrak{X}(\mathsf{M})$$

that for $X \in \mathfrak{X}(\mathsf{M})$ we regard as a map

$$\nabla_X : \mathfrak{X}(\mathsf{M}) \to \mathfrak{X}(\mathsf{M}).$$

It is required to have the following properties:

$$\nabla_{fX+gY} = f\nabla_X + g\nabla_Y, \tag{3.4a}$$

$$\nabla_X(Y + Z) = \nabla_X Y + \nabla_X Z, \tag{3.4b}$$

$$\nabla_X(fY) = \mathscr{L}_X f + f\nabla_X Y, \tag{3.4c}$$

for $X, Y, Z \in \mathfrak{X}(\mathsf{M})$ and $f, g \in \mathfrak{F}(\mathsf{M})$

A connection ∇ is not a tensor field, because it is not linear with respect to functions in its second argument. Also there is no canonical choice of connection on a differentiable manifold. However, we will see that every Riemannian metric has a special connection associated with it.

Definition 3.13. *Let* $\boldsymbol{\gamma} : (a, b) \to \mathsf{M}$ *be curve in a differentiable* M*, and let* ∇ *be a connection on* M*. The* **acceleration** *of* $\boldsymbol{\gamma}$ *with respect to* ∇ *is the vector field*

$$t \longmapsto \nabla_{\boldsymbol{\gamma}'(t)}\boldsymbol{\gamma}'(t),$$

which we write more simply as $\nabla_{\boldsymbol{\gamma}'}\boldsymbol{\gamma}'$*. We say that a curve* $\boldsymbol{\gamma} : (a, b) \to \mathsf{M}$ *is a* **geodesic** *with respect to* ∇ *provided*

$$\nabla_{\boldsymbol{\gamma}'(t)}\boldsymbol{\gamma}'(t) = 0 \tag{3.5}$$

for $a < t < b$*.*

3.2 Riemannian Geometry

The metric properties of $\mathbb{R}^n$ (distances, angles, volumes) are determined by the canonical Cartesian coordinates. In a general differentiable manifold, however, there are no such preferred coordinates; to define distances, angles, and volumes one must add more structure.

Riemannian geometry itself is a vast subject. Here, only the part of it which is important in the subject of mechanics, is discussed. For a detailed account, one should refer [do Carmo 1993] for an example.

Definition 3.14. *A* **Riemannian manifold** *is a pair* (M, g)*, where* M *is a differentiable manifold and* g *is a symmetric*[4]*, positive definite*[5] *2-tensor field (*g *is said to be a* **Riemannian metric** *in* M*).*

A Riemannian metric is therefore a smooth assignment of an inner product to each tangent space. It is usual to write $g_{\mathbf{p}}(v, w) = \langle v, w\rangle_{\mathbf{p}}$.

Proposition 3.2.1. *Let* (N, g) *be Riemannian manifold and* $\Psi : \mathsf{M} \to \mathsf{N}$ *be an* immersion*. Then* $\Psi_{\star\mathbf{p}}g$ *is an* ***induced Riemannian metric*** *in* M *where* $\Psi_{\star\mathbf{p}} : \mathsf{T}_{\mathbf{p}}\mathsf{M} \to \mathsf{T}_{\Psi(\mathbf{p})}\mathsf{N}$ *is the tangent map of* Ψ *at* $\mathbf{p} \in \mathsf{M}$*.*

[4] symmetric if $g(v, w) = g(w, v)$ for all $v, w \in \mathsf{T}_{\mathbf{p}}\mathsf{M}$

[5] positive definite if $g(v, v) > 0$ for all $v \in \mathsf{T}_{\mathbf{p}}\mathsf{M}\backslash\{0\}$

3.2.1 The Levi-Civita affine connection

Of particular interest to this thesis will be a certain affine connection that is determined uniquely from a Riemannian metric g on M.

Definition 3.15. *Let* (M, g) *be a Riemannian manifold. Then the unique* **Levi-Civita affine connection** $\nabla : \mathfrak{X}(\mathsf{M}) \times \mathfrak{X}(\mathsf{M}) \to \mathfrak{X}(\mathsf{M})$ *of* M *is defined by*

$$\begin{aligned} 2\langle \nabla_X Y, Z\rangle &= \mathscr{L}_X\langle Y, Z\rangle + \mathscr{L}_Y\langle X, Z\rangle - \mathscr{L}_Z\langle X, Y\rangle \\ &\quad -\langle X, [Y, Z]\rangle - \langle Y, [X, Z]\rangle + \langle Z, [X, Y]\rangle \end{aligned} \tag{3.6}$$

for $X, Y, Z \in \mathfrak{X}(\mathsf{M})$.

Lemma 3.2.1. *A Riemannian connection* ∇ *has the following properties:*

$$\nabla_{fX+gY} = f\nabla_X + g\nabla_Y, \tag{3.7a}$$
$$\nabla_X(aY + bZ) = a\nabla_X Y + b\nabla_X Z, \tag{3.7b}$$
$$\nabla_X fY = \mathscr{L}_X fY + f\nabla_X Y, \tag{3.7c}$$
$$\nabla_X Y - \nabla_Y X = [X, Y], \tag{3.7d}$$
$$\mathscr{L}_X\langle Y, Z\rangle = \langle \nabla_X Y, Z\rangle + \langle Y, \nabla_X Z\rangle \tag{3.7e}$$

for $X, Y, Z \in \mathfrak{X}(\mathsf{M})$, $f, g \in \mathfrak{F}(\mathsf{M})$ *and* $a, b \in \mathbb{R}$.

3.2.2 The classical treatment of metrics

A frequently used notation for a metric is ds^2. Thus we write the metric as

$$ds^2 = \langle\ ,\ \rangle$$

and is given in terms of the g_{ij}'s by the formula

$$ds^2 = \sum_{ij=1}^{n} g_{ij} dx_i dx_j \tag{3.8}$$

where

$$g_{ij} = \Big\langle \frac{\partial}{\partial x_i}, \frac{\partial}{\partial x_j} \Big\rangle.$$

The **components of the metric** $\langle\ ,\ \rangle$ g_{ij}'s are frequently known as the **lower** g-ij's and the elements of the inverse of the matrix (g_{ij}), denoted (g^{ij}), are called **upper** g-ij's.

Sometimes we need to express the Riemannian connection in terms of local coordinates $(x_1, \ldots x_n)$. Therefore we introduce the **Christoffel symbols** Γ_{ij}^k of ∇ relative to $(x_1, \ldots x_n)$ as

$$\Gamma_{ij}^k = dx_k\left(\nabla_{\frac{\partial}{\partial x_i}}\frac{\partial}{\partial x_j}\right) \tag{3.9}$$

for $1 \leq i, j, k \leq n$. It is an immediate consequence to write the following

$$\nabla_{\frac{\partial}{\partial x_i}}\frac{\partial}{\partial x_j} = \sum_{k=1}^{n}\Gamma_{ij}^k\frac{\partial}{\partial x_k} \tag{3.10}$$

for $1 \leq i, j \leq n$.

It is possible to define the Christoffel symbols for a general connection, discussed in Section 3.1.4, on a differentiable manifold. But the symmetry property

$$\Gamma_{ij}^k = \Gamma_{ji}^k \tag{3.11}$$

may not hold for a general connection. The following classical expression for the Γ_{ij}^k's is used in what follows when we discuss the geometry of the eye movements.

$$\Gamma_{ij}^k = \sum_{h=1}^{n}\frac{g^{ih}}{2}\left\{\frac{\partial g_{hj}}{\partial x_k} + \frac{\partial g_{hk}}{\partial x_j} - \frac{\partial g_{jk}}{\partial x_h}\right\} \tag{3.12}$$

3.2.3 Geodesic equations on a Riemannian manifold

Roughly speaking, a geodesic is a curve whose length is the shortest distance between two points. In the case of a surface $\mathsf{M} \subset \mathbb{R}^n$, if $\boldsymbol{\gamma}$ is a curve in M, there are two notions of acceleration of $\boldsymbol{\gamma}$, namely $\boldsymbol{\gamma}''$ and $\nabla_{\boldsymbol{\gamma}'}\boldsymbol{\gamma}'$, where ∇ is the Riemannian connection of M. $\boldsymbol{\gamma}''$ is known as the $\mathbb{R}^n$-*acceleration* of $\boldsymbol{\gamma}$ and $\nabla_{\boldsymbol{\gamma}'}\boldsymbol{\gamma}'$ is known as the *tangential component* of the $\mathbb{R}^n$-acceleration of $\boldsymbol{\gamma}$. We say that $\boldsymbol{\gamma}$ is a **geodesic** in M when the tangential component of the acceleration of $\boldsymbol{\gamma}$ vanishes, i.e., $\nabla_{\boldsymbol{\gamma}'}\boldsymbol{\gamma}' = 0$ as in the Definition 3.13. A careful account of geodesics is given in [Nishikawa 2001].

3.2.4 Curvature

Definition 3.16. *The* **curvature** $\mathcal{R}$ *of a Riemannian manifold* (M, g) *is a correspondence that associates to every pair* $X, Y \in \mathfrak{X}(\mathsf{M})$ *a mapping* $\mathcal{R}(X,Y) : \mathfrak{X}(\mathsf{M}) \to \mathfrak{X}(\mathsf{M})$ *given by*

$$\mathcal{R}(X,Y)Z = \nabla_Y \nabla_X Z - \nabla_X \nabla_Y Z + \nabla_{[X,Y]} Z, \quad Z \in \mathfrak{X}(\mathsf{M}), \tag{3.13}$$

where ∇ *is the Riemannian connection of* M.

Note that when $\mathsf{M}=\mathbb{R}^n$, $\mathcal{R}(X,Y)Z = 0$ for all $X, Y, Z \in \mathfrak{X}(\mathsf{M})$. Therefore $\mathcal{R}$ can be thought of as a way of measuring how much M deviates from being Euclidean. Also, in coordinates $\{x_i\}$ around $\mathbf{p} \in \mathsf{M}$, we obtain

$$\mathcal{R}(\frac{\partial}{\partial x_i}, \frac{\partial}{\partial x_j})\frac{\partial}{\partial x_k} = \left(\nabla_{\frac{\partial}{\partial x_j}} \nabla_{\frac{\partial}{\partial x_i}} - \nabla_{\frac{\partial}{\partial x_i}} \nabla_{\frac{\partial}{\partial x_j}}\right)\frac{\partial}{\partial x_k}, \quad \text{since } \left[\frac{\partial}{\partial x_i}, \frac{\partial}{\partial x_j}\right] = 0$$

i.e., the curvature measures the non-commutativity of the covariant derivative.

It is sometimes convenient to express $\mathcal{R}$ in terms of the coordinates. Let $\frac{\partial}{\partial x_i} = \partial_{x_i}$, then

$$\mathcal{R}(\partial_{x_i}, \partial_{x_j})\partial_{x_k} = \sum_\ell \mathcal{R}^\ell_{ijk} \partial_{x_\ell}$$

If

$$X = \sum_i u^i \partial_{x_i}, \; Y = \sum_i v^i \partial_{x_i}, \; Z = \sum_i w^i \partial_{x_i},$$

$\mathcal{R}$ can be written as

$$\mathcal{R}(X,Y)Z = \sum_{i,j,k,\ell} \mathcal{R}^\ell_{ijk} u^i v^j w^k \partial_{x_\ell} \tag{3.14}$$

where

$$\mathcal{R}^s_{ijk} = \sum_\ell \Gamma^\ell_{ik}\Gamma^s_{j\ell} - \sum_\ell \Gamma^\ell_{jk}\Gamma^s_{i\ell} + \partial_{x_j}\Gamma^s_{ik} - \partial_{x_i}\Gamma^s_{jk} \tag{3.15}$$

3.3 Quaternions to represent rotations

In 1843, Hamilton discovered the *quaternions* which are hyper-complex numbers[6] of rank 4 together with the crucial rule $\overrightarrow{\mathbf{i}}^2 = \overrightarrow{\mathbf{j}}^2 = \overrightarrow{\mathbf{k}}^2 = \overrightarrow{\mathbf{i}}\,\overrightarrow{\mathbf{j}}\,\overrightarrow{\mathbf{k}} = -1$. The set of quaternions, along with the two operations of addition and multiplication, form

[6] real numbers can be treated as hyper-complex numbers of rank 1, and *ordinary* complex numbers as being hyper-complex numbers of rank 2.

a mathematical system called a *ring*, more precisely a *non-commutative division ring*. Thus, the quaternion product, in general, is not commutative, and the multiplicative inverse exists for every non-zero element in the set. Here, we discuss the use of quaternions to represent rotations. Listing's law can be well understood with this setting. For a thorough discussion of the topic of quaternions one should refer [Kuipers 1998], and [Conway & Smith 2003].

Space of quaternions are denoted by $\mathbf{Q}$. We write each $a \in \mathbf{Q}$ as $a_0\overrightarrow{\mathbf{1}} + a_1\overrightarrow{\mathbf{i}} + a_2\overrightarrow{\mathbf{j}} + a_3\overrightarrow{\mathbf{k}}$, call $a_1\overrightarrow{\mathbf{i}} + a_2\overrightarrow{\mathbf{j}} + a_3\overrightarrow{\mathbf{k}}$ its vector part, and $a_0\overrightarrow{\mathbf{1}}$ its scalar part. The vector $a_1\overrightarrow{\mathbf{i}} + a_2\overrightarrow{\mathbf{j}} + a_3\overrightarrow{\mathbf{k}}$ will be identified with $(a_1, a_2, a_3) \in \mathbb{R}^3$ without any explicit mention of it. When there is no confusion we drop $\overrightarrow{\mathbf{1}}$ from the scalar part, and simply write it as a_0. The vector part of a quaternion a will be denoted by $\mathbf{vec}(a)$, or simply by $\mathbf{a}$, and the scalar part will be denoted by $\mathbf{scal}$(a). Thus we have maps,

$$\mathbf{vec} : \mathbf{Q} \to \mathbb{R}^3, \;\; a \mapsto \mathbf{a} = (a_1, a_2, a_3),$$

and

$$\mathbf{scal} : \mathbf{Q} \to \mathbb{R}, \;\; a \mapsto a_0.$$

Operations on quaternions: Consider two quaternions $p = p_0 + \mathbf{p}$ and $q = q_0 + \mathbf{q}$.

$$\begin{aligned}
p.q &= p_0q_0 - \mathbf{p} \,.\, \mathbf{q} + p_0\mathbf{q} + q_0\mathbf{p} + \mathbf{p} \times \mathbf{q} && \text{(quaternion product)}\\
p^\star &= p_0 - \mathbf{p} && \text{(conjugate of a quaternion)}\\
p \,.\, q &= \mathbf{scal}(p.q^\star) && \text{(dot product of quaternions)}\\
|p| &= \sqrt{p^\star.p} = \sqrt{p_0^2 + \mathbf{p} \,.\, \mathbf{p}} && \text{(norm of a quaternion)}\\
p^{-1} &= p^\star/|p| && \text{(inverse of a quaternion)}
\end{aligned}$$

Space of unit quaternions will be identified with the unit sphere embedded in $\mathbb{R}^4$, and denoted by S^3. The unit quaternions form the group $\mathsf{SU}(2)$, the group of unitary rotations, which is the *double covering* of the rotation group $\mathsf{SO}(3)$. Thus, they suite well for the study of rotations. Note that for a unit quaternion q, $q^{-1} = q^\star$.

Each $q \in S^3$ can be written as $q = cos(\alpha/2)\overrightarrow{\mathbf{1}} + sin(\alpha/2)n_1\overrightarrow{\mathbf{i}} + sin(\alpha/2)n_2\overrightarrow{\mathbf{j}} + sin(\alpha/2)n_3\overrightarrow{\mathbf{k}}$, where, $\alpha \in [0, \pi]$ and $\hat{\mathbf{n}} = (n_1, n_2, n_3)$ is a unit vector in $\mathbb{R}^3$. The notation $q = \cos(\alpha/2) + \hat{\mathbf{n}}\sin(\alpha/2)$ where $\hat{n} = n_1\overrightarrow{\mathbf{i}} + n_2\overrightarrow{\mathbf{j}} + n_3\overrightarrow{\mathbf{k}}$, is also used interchangeably.

Theorem 3.3.1. *For a unit quaternion* $q = \cos(\alpha/2) + \hat{\mathbf{n}}\sin(\alpha/2)$*, the map* $\mathbf{v} \to q.\mathbf{v}.q^{-1}$ *represents a* **simple rotation** *of a vector* $\mathbf{v}$ *by an angle* α *about the axis* $\hat{\mathbf{n}}$*, in Euclidean 3-space.*

See Appendix A for a proof of this theorem.

We denote by **rot** the standard map from S^3 into $\mathsf{SO}(3)$, i.e., $\mathbf{rot} : S^3 \to \mathsf{SO}(3)$ which maps $cos(\alpha/2)\overrightarrow{\mathbf{1}} + sin(\alpha/2)n_1\overrightarrow{\mathbf{i}} + sin(\alpha/2)n_2\overrightarrow{\mathbf{j}} + sin(\alpha/2)n_3\overrightarrow{\mathbf{k}}$ to a rotation around the axis $\hat{\mathbf{n}}$ by a counterclockwise angle α. There are two explicit ways of describing this map. First, it is easy to verify that

$$\mathbf{rot}(q)(v_1, v_2, v_3) = \mathbf{vec}(q.(v_1\overrightarrow{\mathbf{i}} + v_2\overrightarrow{\mathbf{j}} + v_3\overrightarrow{\mathbf{k}}).q^{-1}).$$

Second (see Equation (A.2)),

$$\mathbf{rot}(q) = \begin{bmatrix} q_0^2 + q_1^2 - q_2^2 - q_3^2 & 2(q_1q_2 - q_0q_3) & 2(q_1q_3 + q_0q_2) \\ 2(q_1q_2 + q_0q_3) & q_0^2 + q_2^2 - q_1^2 - q_3^2 & 2(q_2q_3 - q_0q_1) \\ 2(q_1q_3 - q_0q_2) & 2(q_2q_3 + q_0q_1) & q_0^2 + q_3^2 - q_1^2 - q_2^2 \end{bmatrix}.$$

Space of rotations can be thought of as the unit sphere in $\mathbb{R}^4$ with antipodal points identified ($-q$ represents the same rotation as q). In the standard language, the set of unit quaternions is a double cover of $\mathsf{SO}(3)$, as we already mentioned earlier. Thus, **rot** is a 2-to-1 homomorphism[7].

[7]If G and H are groups, then a group homomorphism of G into H is a function $\Phi : G \to H$ which preserves the group operation, i.e., for all $g_1, g_2 \in G$, $(g_1g_2)\Phi = (g_1)\Phi(g_2)\Phi$

Chapter 4

Mechanical Control Systems

Mechanics is the paradise of the mathematical sciences, because by means of it one comes to the fruits of mathematics.

— Leonardo da Vinci

This chapter is an introduction to "geometric mechanics" where we make use of the ideas discussed in the previous chapter. Among many different problems, mechanics deals with rigid body movements. In the treatment discussed in this thesis on eye movements, eye is treated as a rigid sphere free to move inside the "socket" which consists of the orbital tissues.

Over the years, mechanics and mathematics benefitted from each other. As calculus was evolved due to Newtonian mechanics, the modern results in geometry and topology play a key role in current developments in many engineering problems. There is an exciting mass of literature available on this subject (see [Smale 1970*a*, Smale 1970*b*], [Brockett 1982], [Krishnaprasad et al. 1991], [Yang, Krishnaprasad & Dayawansa 1996] etc.). Textbooks, such as [Arnol'd 1989] gives a good introduction while [Abraham & Marsden 1987], [Marsden & Ratiu 1999] and [Bullo & Lewis 2004] discuss more advanced topics. Less geometric treatment of mechanics (known as "classical mechanics") can be found in [Goldstein 1980].

In studying the eye movement system, we consider the so-called ***simple mechanical control systems*** [Smale 1970*a*, Smale 1970*b*]. Such systems consist the following:

- a ***configuration manifold*** Q,

- Riemannian metric g on Q that defines the kinetic energy function on the tangent bundle of Q,
- external forces as possibly time-dependent cotangent bundle-valued functions on the tangent bundle,
- any constraints on the system,
- control forces on the system as covector fields on the configuration manifold.

4.1 The configuration manifold

The first step in the geometric approach to mechanical systems is to assign a differentiable manifold, as the configuration manifold $\mathbf{Q}$, that has 1-1 correspondence with the configuration of the system. Since this may not be Euclidean, it poses a problem when describing the dynamics of the system. Thus the next step is to assign a ***coordinate chart*** which describes the precise manner in which points in Q correspond to configurations of the physical system. Let's consider an example.

Example 4.1.1: *A particle moving on a circle of radius r.*
Configuration space for this problem would be

$$\mathsf{Q} = S^1 = \{x \in \mathbb{R}^2 \mid \|x\| = 1\}.$$

Indeed, the radius of the circle is r. However, the configuration space is typically chosen to be some dimensionless object, and the physics of the problem, i.e., r in this case, is included into other aspects of the problem description.
Choose a coordinate chart $(\mathbf{x}, \mathcal{U})$ for $\mathsf{Q} = S^1$ as follows:

$$\mathbf{x}(t) = (x, y) = \tan(t)$$

and

$$t \in \mathcal{U} = (-\pi, \pi) \subset \mathbb{R}, \text{ and } \mathbf{x}(\mathcal{U}) = S^1 \setminus \{(-1, 0)\} \subset S^1$$

Here $\tan : (-\pi, \pi] \to \mathbb{R}^2 \setminus \{(0, 0)\}$, where $t \in (-\pi, \pi)$ is the usual angle measured so that $\tan(0) = (x, 0)$ for $x > 0$.

4.2 Kinetic energy and Riemannian metric

In this section we discuss how to obtain a Riemannian metric for the configuration manifold. This is achieved by defining the kinetic energy for the system as a function on the tangent bundle of the configuration manifold. Therefore, it is necessary to first introduce the inertia tensor for a rigid body.

A ***rigid body*** is a pair $(\mathcal{B}, \mu)$, where $\mathcal{B} \subset \mathbb{R}^3$ is compact and μ is a finite measure[1] on $\mathbb{R}^3$ called the ***mass distribution***. Therefore the ***mass*** is written as

$$\mu(\mathcal{B}) = \int_{\mathcal{B}} \mathrm{d}\mu$$

The ***center of mass*** of a rigid body is the point

$$\boldsymbol{\xi}_c = \frac{1}{\mu(\mathcal{B})} \left(\int_{\mathcal{B}} \boldsymbol{\xi} \mathrm{d}\mu \right).$$

The ***inertia tensor about*** $\boldsymbol{\xi}_0$ of $(\mathcal{B}, \mu)$ is the linear map $\mathbb{I}_{\boldsymbol{\xi}_0} \in L(\mathbb{R}^3; \mathbb{R}^3)$ given by

$$\mathbb{I}_{\boldsymbol{\xi}_0}(\boldsymbol{v}) = \int_{\mathcal{B}} (\boldsymbol{\xi} - \boldsymbol{\xi}_0) \times (\boldsymbol{v} \times (\boldsymbol{\xi} - \boldsymbol{\xi}_0)) \mathrm{d}\mu. \tag{4.1}$$

About the center of mass of $(\mathcal{B}, \mu)$, it is denoted by $\mathbb{I}_c$. The inertia tensor is symmetric with respect to the inner product $(\ ,\ )_{\mathbb{R}^3}$, i.e.,

$$(\mathbb{I}_{\boldsymbol{\xi}_0}(\boldsymbol{v}_1), \boldsymbol{v}_2)_{\mathbb{R}^3} = (\boldsymbol{v}_1, \mathbb{I}_{\boldsymbol{\xi}_0}(\boldsymbol{v}_2))_{\mathbb{R}^3}\,.$$

Thus the eigenvalues of the inertia tensor $\mathbb{I}_c$ are real and let's denote them as $\{J_1, J_2, J_3\}$. These are called the ***principal inertias*** of $(\mathcal{B}, \mu)$. The orthonormal eigenvectors associated with these eigenvalues, are called ***principal axes*** of $(\mathcal{B}, \mu)$.

4.2.1 Kinetic energy of a rigid body

The rotational motion of a rigid body $(\mathcal{B}, \mu)$ may be described by the geodesic flow of a given left-invariant metric on $\mathsf{SO}(3)$, the group of linear orthogonal orientation-preserving transformations of $\mathbb{R}^3$, or, equivalently, with the group of

[1] one may replace μ by ρdV, where $\rho : \mathcal{B} \to \mathbb{R}$ is the "mass density"

3×3 orthogonal unimodular matrices:

$$\begin{aligned} \mathsf{SO}(3) &= \{\boldsymbol{R} : \mathbb{R}^3 \to \mathbb{R}^3 \mid (\boldsymbol{R}x, \boldsymbol{R}y)_{\mathbb{R}^3} = (x, y)_{\mathbb{R}^3}\,,\ \det \boldsymbol{R} = 1\} \\ &= \{\boldsymbol{R} : \mathbb{R}^3 \to \mathbb{R}^3 \mid \boldsymbol{R}\boldsymbol{R}^T = \mathrm{Id},\ \det \boldsymbol{R} = 1\} \end{aligned}$$

We denote above the standard inner product in $\mathbb{R}^3$ by $(.,.)_{\mathbb{R}^3}$.

The metric is determined by the body's inertia tensor. Let the inertia tensor of the rigid body $(\mathcal{B}, \mu)$ about the center of mass, be $\mathbb{I}_c$. Here, we generalize the usual notation $\frac{1}{2}m\|\dot{\boldsymbol{x}}\|^2_{\mathbb{R}^3}$ for a particle. That is, treating the mechanical system as a collection of particles and summing up.

Consider a rigid body that is free to rotate about a fixed point. Let $\{\mathcal{O}_{\text{inertial}} - \boldsymbol{e}_1, \boldsymbol{e}_2, \boldsymbol{e}_3\}$ be the orthonormal inertial frame and $\{\mathcal{O}_{\text{body}} - \boldsymbol{b}_1, \boldsymbol{b}_2, \boldsymbol{b}_3\}$ be the orthonormal body frame fixed at its center of mass. For convenience, let's take the origins of both frames $\mathcal{O}_{\text{body}}, \mathcal{O}_{\text{inertial}}$ to be the origin of $\mathbb{R}^3$, and by their relative orientation $\boldsymbol{R} \in \mathsf{SO}(3)$. Therefore the movement can be described by a curve $t \mapsto \boldsymbol{R}(t) \in \mathsf{SO}(3)$, i.e., a point $\boldsymbol{\xi} \in \mathcal{B}$ at time t is given by $\boldsymbol{x}(t, \boldsymbol{\xi}) = \boldsymbol{R}(t)\boldsymbol{\xi}$. Therefore the kinetic energy of the body at time t is given by

$$K(t) = \frac{1}{2}\int_{\mathcal{B}} \|\dot{\boldsymbol{x}}(t, \boldsymbol{\xi})\|^2 \mathrm{d}\mu = \frac{1}{2}\int_{\mathcal{B}} \|\dot{\boldsymbol{R}}(t)\boldsymbol{\xi}\|^2 \mathrm{d}\mu.$$

The body ***angular velocity*** is defined as

$$\boldsymbol{\Omega}(t) = \boldsymbol{R}^T(t)\dot{\boldsymbol{R}}(t). \tag{4.2}$$

This is a skew-symmetric matrix. To see that, differentiate $\boldsymbol{R}^T(t)\boldsymbol{R}(t) = \boldsymbol{I}_3$

$$\dot{\boldsymbol{R}}(t)\boldsymbol{R}(t) + \boldsymbol{R}^T(t)\dot{\boldsymbol{R}}(t) = \boldsymbol{0}$$

giving what is required,

$$\boldsymbol{\Omega}^T(t) = (\boldsymbol{R}^T(t)\dot{\boldsymbol{R}}(t))^T = -\boldsymbol{R}^T(t)\dot{\boldsymbol{R}}(t) = \boldsymbol{\Omega}(t).$$

Thus the velocities of the rigid body have the form

$$\dot{\boldsymbol{R}}(t) = \boldsymbol{R}(t)\boldsymbol{\Omega}(t), \qquad \boldsymbol{\Omega}^T(t) = -\boldsymbol{\Omega}(t). \tag{4.3}$$

In other words, we found the tangent space

$$\mathsf{T}_{\boldsymbol{R}}\mathsf{SO}(3) = \{\boldsymbol{R}\boldsymbol{\Omega} \mid \boldsymbol{\Omega}^T = -\boldsymbol{\Omega}\}, \qquad \boldsymbol{R} \in \mathsf{SO}(3). \tag{4.4}$$

Denote the space of antisymmetric 3×3 matrices by $so(3)$, i.e., it is the tangent space to $\mathsf{SO}(3)$ at the identity:

$$so(3) = \{\boldsymbol{\Omega} : \mathbb{R}^3 \to \mathbb{R}^3 \mid \boldsymbol{\Omega}^T = -\boldsymbol{\Omega}\} = \mathsf{T}_{\mathrm{Id}}\mathsf{SO}(3). \tag{4.5}$$

Note that the space $so(3)$ is the Lie algebra[2] of the Lie group $\mathsf{SO}(3)$.

Let

$$\boldsymbol{\Omega} \sim \boldsymbol{\omega}(t) \qquad \boldsymbol{\Omega}(t) = \begin{bmatrix} 0 & -\omega_3(t) & \omega_2(t) \\ \omega_3(t) & 0 & -\omega_1(t) \\ -\omega_2(t) & \omega_1(t) & 0 \end{bmatrix} \qquad \boldsymbol{\omega}(t) = \begin{bmatrix} \omega_1(t) \\ \omega_2(t) \\ \omega_3(t) \end{bmatrix} \in \mathbb{R}^3. \tag{4.6}$$

Then one can verify that $\boldsymbol{\Omega}(t)\boldsymbol{v} = \boldsymbol{\omega}(t) \times \boldsymbol{v}$. For a point x in the rigid body its position in $\mathbb{R}^3$ is $\boldsymbol{R}(t)x$. Therefore the velocity of this point is $\dot{\boldsymbol{R}}(t)x = \boldsymbol{R}(t)\boldsymbol{\Omega}(t)x = \boldsymbol{R}(t)(\boldsymbol{\omega}(t) \times x)$, i.e., the point x rotates around the line through $\boldsymbol{\omega}(t)$ with the angular velocity $\|\boldsymbol{\omega}(t)\|$.

Introduce the following scalar product of matrices $\boldsymbol{\Omega} = (\Omega_{ij}) \in so(3)$:

$$\left\langle \boldsymbol{\Omega}^1, \boldsymbol{\Omega}^2 \right\rangle = -\frac{1}{2}\mathrm{tr}(\boldsymbol{\Omega}^1\boldsymbol{\Omega}^2) = \frac{1}{2}\sum_{i,j=1}^{3} \Omega^1_{ij}\Omega^2_{ij} = \sum_{i<j} \Omega^1_{ij}\Omega^2_{ij}. \tag{4.7}$$

This product is compatible with 3×3 antisymmetric matrices and 3-dimensional vectors in (4.6):

$$\begin{gathered} \left\langle \boldsymbol{\Omega}^1, \boldsymbol{\Omega}^2 \right\rangle = \left(\boldsymbol{\omega}^{\mathbf{1}}, \boldsymbol{\omega}^{\mathbf{2}}\right)_{\mathbb{R}^3}, \\ \boldsymbol{\Omega}^i \sim \boldsymbol{\omega}^i, \qquad \boldsymbol{\Omega}^i \in so(3), \qquad \boldsymbol{\omega}^i \in \mathbb{R}^3, \quad i = 1, 2. \end{gathered} \tag{4.8}$$

Returning to the expression of kinetic energy, we have

$$K(t) = \frac{1}{2}\int_{\mathcal{B}} \|\dot{\boldsymbol{R}}(t)\boldsymbol{\xi}\|^2 \mathrm{d}\mu = \frac{1}{2}\int_{\mathcal{B}} \|\boldsymbol{R}(t)(\boldsymbol{\omega} \times \boldsymbol{\xi})\|^2 \mathrm{d}\mu$$

[2] i.e., the tangent space to the Lie group at the identity provided with the Lie bracket $[\ ,\ ]$

$$
\begin{aligned}
K(t) &= \frac{1}{2}\int_{\mathcal{B}} \|(\boldsymbol{\omega}\times\boldsymbol{\xi})\|^2 \mathrm{d}\mu = \frac{1}{2}\int_{\mathcal{B}} (\boldsymbol{\omega}\times\boldsymbol{\xi}, \boldsymbol{\omega}\times\boldsymbol{\xi})_{\mathbb{R}^3}\, \mathrm{d}\mu \\
&= \frac{1}{2}\int_{\mathcal{B}} (\boldsymbol{\xi}\times(\boldsymbol{\omega}(t)\times\boldsymbol{\xi}), \boldsymbol{\omega}(t))_{\mathbb{R}^3}\, \mathrm{d}\mu \quad \text{(Using the result } (u, v\times w) = (w, u\times v)\text{)} \\
&= \frac{1}{2}(\mathbb{I}_c(\boldsymbol{\omega}(t)), \boldsymbol{\omega}(t))_{\mathbb{R}^3} \qquad \text{(Using Eq. (4.7))} \\
&= \frac{1}{2}\langle \boldsymbol{\Omega}, \boldsymbol{\Omega}\rangle_I \qquad \text{(Using Eq. (4.8))}
\end{aligned}
$$

Example 4.2.1 (Falling cat): A popular example of the generation of rotational motion is the falling cat, which is able to execute a 180^0 reorientation, all the while having zero angular momentum. It achieves this by manipulating its joints to create shape changes. Considering that the angular momentum of a rotating rigid object is its moment of inertia times its instantaneous angular velocity; shape changes result in a change in the cat's moment of inertia and this, together with the constancy of the angular momentum, creates the overall orientation change.

4.2.2 Riemannian metric on the configuration space

In order to obtain the Riemannian metric on the configuration manifold Q, it is required to define a $(0,2)$-tensor field on Q. Let us define a C^∞ map

$$\rho : \mathsf{Q} \to \mathsf{SO}(3).$$

If $\gamma : I \to \mathsf{Q}$ is a curve at $q_0 \in \mathsf{Q}$, there will be an induced curve on $\mathsf{SO}(3)$ given by $\gamma_\rho = \rho\circ\gamma : I \to \mathsf{SO}(3)$ at $\boldsymbol{R}_0 \in \mathsf{SO}(3)$. The curve γ_ρ then defines the corresponding kinetic energy, i.e., one can assign a positive number $K(v_0)$ to the tangent vector $v_0 = \gamma'(0) \in \mathsf{T}_{q_0}\mathsf{Q}$ at time 0 along γ_ρ. This indeed is a positive-definite $(0,2)$-tensor field on Q that we term as ***kinetic energy metric***.

Example 4.2.2: For a perfect sphere with moment of inertia $I_{3\times3}$, the left-invariant Riemannian metric on $\mathsf{SO}(3)$ is given by

$$\Big\langle \boldsymbol{\Omega}(\boldsymbol{e}_i), \boldsymbol{\Omega}(\boldsymbol{e}_j)\Big\rangle_I = \delta_{i,j} \tag{4.9}$$

where,

$$\mathbf{\Omega}(e_k) = \begin{bmatrix} 0 & \delta_{3,k} & -\delta_{2,k} \\ -\delta_{3,k} & 0 & \delta_{1,k} \\ \delta_{2,k} & -\delta_{1,k} & 0 \end{bmatrix},$$

and $\{\delta_{l,m}\}$ denotes the Kronecker delta function.

4.3 Lagrangian and Hamiltonian formulations

Lagrangian mechanics and ***Hamiltonian mechanics*** are the two main points of view in mechanics. Lagrangian formalism is based on the variational principal one finds in the calculus of variations. The starting point is the the work of [Abraham & Marsden 1987], [Arnol'd 1989] which treats the configuration space as a differentiable manifold. The Hamiltonian formalism is based on the energy concept. Each formalism provides advantages in problems in mechanics and circumstances often dictate which, if any, approach is best. One should refer [Abraham & Marsden 1987], [Marsden & Ratiu 1999], [Arnol'd 1989] etc, for further account of the subject.

4.3.1 Lagrangian mechanics

Let Q be a C^∞-differentiable manifold. A ***Lagrangian*** is a C^∞-function L on $\mathbb{R}\times\mathsf{TQ}$, i.e., a function of time, position and velocity. It is ***time-independent*** if there exists a function $L_0 : \mathsf{TQ} \to \mathbb{R}$ such that $L(t, v_q) = L_0(v_q)$. Most Lagrangians we encounter are of time-independent nature.

The Lagrangian formulation of mechanics relies on the fact that there are variational principles behind the Newton's law $\mathbf{F} = m\mathbf{a}$. If $(\phi, \mathcal{U})$ is a chart for Q with coordinates $(q^1, \ldots, q^n)$, the Lagrangian is written as $L(t, q^1, \ldots, q^n, \dot{q}^1, \ldots, \dot{q}^n)$, or $L(t, \boldsymbol{q}, \dot{\boldsymbol{q}})$ for short. Usually L is the kinetic energy *minus* the potential energy of the system. The ***variational principle of Hamilton*** states

$$\delta \int_a^b L(t, \boldsymbol{q}, \dot{\boldsymbol{q}}) = 0 \tag{4.10}$$

where we choose curves $q^i(t)$ joining two fixed points in Q over a fixed time interval $[a, b]$ and calculate the integral regarded as a function of this curve. Hamilton's principle says that this function has a critical point. Let δq^i be a variation and (4.10) is equivalent to

$$\begin{aligned} \sum_{i=1}^{n} \int_a^b \left(\frac{\partial L}{\partial q^i} \delta q^i + \frac{\partial L}{\partial \dot{q}^i} \delta \dot{q}^i \right) \mathrm{d}t = 0 \\ \sum_{i=1}^{n} \int_a^b \left[\frac{\partial L}{\partial q^i} - \frac{d}{dt} \left(\frac{\partial L}{\partial \dot{q}^i} \right) \right] \delta q^i \mathrm{d}t = 0 \end{aligned} \tag{4.11}$$

This leads to the ***Euler-Lagrange equations***

$$\frac{d}{dt} \frac{\partial L}{\partial \dot{q}^i} - \frac{\partial L}{\partial q^i} = 0, \quad i = 1, \ldots, n. \tag{4.12}$$

An interesting geometric result can be obtained when one considers the kinetic energy Lagrangian

$$L(\boldsymbol{q}, \dot{\boldsymbol{q}}) = \frac{1}{2} \langle \dot{\boldsymbol{q}}, \dot{\boldsymbol{q}} \rangle ,$$

which gives rise to the *equations of geodesics*.

Forces

The Euler-Lagrange equations for a Lagrangian L represents the motion of the system in the absence of the external interactions or forces. Unlike in Newtonian mechanics, the "geometric representation" of a force is less clear in Lagrangian mechanics.

A ***C^r-force*** on a C^r-manifold Q is a map $F : \mathbb{R} \times \mathsf{TQ} \to \mathsf{T}^\star\mathsf{Q}$. We call it ***time-independent*** if there exists a map $F_0 : \mathsf{TQ} \to \mathsf{T}^\star\mathsf{Q}$ with the property that $F(t, v_q) = F_0(v_q)$. A ***C^r-force along γ*** is a C^r-covector field $F : I \to \mathsf{T}^\star\mathsf{Q}$ along a C^r-curve $\gamma : I \to \mathsf{Q}$. If $(q^1, \ldots, q^n)$ are coordinates in a chart $(\phi, \mathcal{U})$, then we write $F = F_i \mathrm{d}q^i$, for some functions $F_i : \mathbb{R} \times \mathsf{T}\mathcal{U} \to \mathbb{R}$, $i \in \{1, \ldots, n\}$, called the ***components*** of the force F. The following principle enables us to formulate the Lagrangian system to include forces.

Lagrange-D'alembert principle: The solution $\gamma : I \to \mathsf{Q}$ to the *simple mechanical control system* satisfies the variational principle

$$\delta \int_I \underbrace{\left(\frac{1}{2}\|\gamma'\|^2 - V(\gamma)\right)}_{\text{Lagrangian } L} \mathrm{d}t + \int_I \langle F(t), \delta q \rangle = 0$$

where the variation δq is an arbitrary vector field along γ.

Note: Systems subject to no force follow geodesics, i.e., $\delta \int_I \|\gamma'\|^2 \mathrm{d}t = 0 \iff \nabla_{\gamma'}\gamma' = 0$.

The Lagrange-D'alembert principle tells us how a force F should appear in the Euler-Lagrange equations.

Proposition 4.3.1 (Forced Euler-Lagrange equations). *Let L be a Lagrangian on Q with F a force on Q. A curve $\gamma : [a, b] \to \mathsf{Q}$ satisfies the Lagrange-D'alembert principle for the force F and Lagrangian L if and only if for any coordinate chart $(\phi, \mathcal{U})$ that intersects the image of γ, the coordinate representation $t \mapsto (q^1, \ldots, q^n)$ satisfies the* ***forced Euler-Lagrange equations***

$$\frac{d}{dt}\frac{\partial L}{\partial \dot{q}^i} - \frac{\partial L}{\partial q^i} = F_i, \quad i = 1, \ldots, n. \tag{4.13}$$

where $F_1, \ldots, F_n$ are the components of F.

Potential forces

A ***potential force***, given a potential function V on Q, is given by $F(t, v_q) = -\mathrm{d}V(q)$. These are independent of time and velocity. Potential function V can be thought of as a "storage function", since by increasing its value one can store energy which could later become kinetic energy.

4.3.2 Hamiltonian mechanics

Hamiltonian formalism is obtained by introducing the ***conjugate momenta***

$$p_i = \frac{\partial L}{\partial \dot{q}^i}, \quad i = 1, \ldots, n, \tag{4.14}$$

and making the change of variables $(q^i, \dot{q}^i) \mapsto (q^i, p_i)$ using the *Legendre transform* to introduce the ***Hamiltonian***

$$\mathcal{H}(q^i, p_i, t) = \sum_{j=1}^{n} p_j \dot{q}^j - L(q^i, \dot{q}^i, t). \tag{4.15}$$

Then

$$\frac{\partial \mathcal{H}}{\partial p_i} = \dot{q}^i + \sum_{j=1}^{n} \left(p_j \frac{\partial \dot{q}^j}{\partial p_i} - \frac{\partial L}{\partial \dot{q}^j} \frac{\partial \dot{q}^j}{\partial p_i} \right) = \dot{q}^i$$

and

$$\frac{\partial \mathcal{H}}{\partial q_i} = \sum_{j=1}^{n} p_j \frac{\partial \dot{q}^j}{\partial q^i} - \frac{\partial L}{\partial q^i} - \sum_{j=1}^{n} \frac{\partial L}{\partial \dot{q}^j} \frac{\partial \dot{q}^j}{\partial q^i} = -\frac{\partial L}{\partial q^i}.$$

Using (4.12), the above reduces to

$$\frac{\partial \mathcal{H}}{\partial q^i} = -\dot{p}_i.$$

Therefore the *Euler-Lagrange equations* are equivalent to ***Hamilton's equations***

$$\begin{aligned} \dot{q}^i &= \frac{\partial \mathcal{H}}{\partial p_i}, \\ \dot{p}_i &= -\frac{\partial \mathcal{H}}{\partial q^i}, \end{aligned} \tag{4.16}$$

where $i = 1, \ldots, n$.

Holonomic and nonholonomic constraints

Many mechanical systems are obtained from higher-dimensional ones by adding constraints. Rigidity in rigid-body mechanics, incompressibility in fluid mechanics and a particle constrained to move on a sphere are few examples for such systems. The eye movement system, as we show in Chapter 6, is another example.

Constraints on a mechanical system are two-fold. ***Holonomic*** constraints are those imposed on the configuration space of the system which are generally integrable. Constraints involving the conditions on the velocity that are non-integrable, are termed ***nonholonomic***. A rolling disk without slipping is an example for such a system. A velocity constraint $\mathcal{D}$ can be holonomic, if all curves through a point $q \in \mathsf{Q}$ satisfying the constraint are evolving on the maximal

integral manifold for $\mathcal{D}$ through q. In such an event, one should restrict one's consideration to maximal integral manifold. This may not be possible sometimes, for an example, if the maximal integral manifold is not a submanifold.

A holonomic constraint can be defined for our purposes as the specification of a submanifold $N \subset \mathsf{Q}$ of a given configuration manifold Q. Precisely, a holonomic constraint is an integrable subbundle of TQ. Thus given a Lagrangian $L : \mathsf{TQ} \to \mathbb{R}$, it can be restricted to TN to give a Lagrangian L_{N} and one can associate variational principles and Hamiltonian vector fields.

4.4 Maximum Principle

After forty years from its first publication, the ***Pontryagin Maximum Principle (PMP)*** [Pontryagin, Boltyanskii, Gamkrelidze & Mishchenko 1964] remains as the most powerful tool in the study of optimal control problems. Recent generalizations of PMP with a geometric setting has been discussed in [Sussman 1998, Sussman & Willems 2000].

Here, a control system is viewed as a dynamical system whose dynamical laws are not entirely fixed, but depend on the controls that can be determined in order to obtain a temporal evolution with some properties. It is assumed that the configuration space is a smooth manifold M. The motion on M follows a number of tangent directions, depending on the control $u : [a, b] \to U \subset \mathbb{R}^m$:

$$\dot{x}(t) = f(x(t), u(t)), \quad x \in \mathsf{M}. \tag{4.17}$$

Problem 4.4.1: Find a pair $(u(t), x(t))$ that minimizes the functional

$$J(u, x) = \int_a^b L(x(t), u(t))\mathrm{d}t,$$

subject to $\dot{x}(t) = f(x(t), u(t))$, $x(a) = x_0$ and $x(b) = x_1$, where $x(t)$ is a curve on the state manifold M, $u : [a, b] \to U \subset \mathbb{R}^m$ is a measurable function, and $L(x, u) \in C^\infty(M \times \mathbb{R}^m)$

The system in (4.17) puts a restriction on our admissible curves. Given the Lagrangian $L(x, u)$, one defines the ***Hamiltonian***

$$\mathcal{H}(x, \lambda, u) = \lambda . f(x, u) - \lambda_0 L(x, u).$$

$\lambda_0 \in \{0, 1\}$ is known as the *abnormal multiplier*.

The necessary condition is given in [Pontryagin et al. 1964] to minimize J with the restriction of equation (4.17).

Theorem 4.4.1 (PMP). *A necessary condition for the pair $(u(t), x(t))$ to solve Problem 4.4.1 is that there exist a one-form field $\lambda(t)$ along $x(t)$ and a constant $p_0 \in \{0, 1\}$ such that*

1. $(\lambda(t), \lambda_0) \neq (0, 0)$ *for all* $t \in [a, b]$,
2. $\dot{x}(t) = \frac{\partial \mathcal{H}}{\partial \lambda}(x(t), \lambda(t), u(t))$ *and* $\dot{\lambda}(t) = \frac{\partial \mathcal{H}}{\partial x}(x(t), \lambda(t), u(t))$ *for all* $t \in [a, b]$,
3. $\mathcal{H}(x(t), \lambda(t), u(t)) = \max_{\tilde{u} \in U} \mathcal{H}(x(t), \lambda(t), \tilde{u}(t))$ *for all* $t \in [a, b]$,
4. $\mathcal{H}(x, \lambda, u) = \lambda . f(x, u) - \lambda_0 L(x, u)$ *is constant almost everywhere along the solutions and if we allow the end points to vary, this constant may be chosen to be zero.*

PMP is indeed a first order necessary condition for optimality. Once the target is set as the attainable set from x_0, one can obtain a family of optimal trajectories. If $u(t)$ is an admissible control and $\lambda(t)$ a Lipschitizian[3] curve in $\mathsf{T}^\star\mathsf{M}$ satisfying PMP, then $\lambda(t)$ is called an *extremal*. PMP provides a lift to the cotangent bundle, that is, a solution to a suitable pseudo-Hamiltonian system. The whole set of extremals in the cotangent bundle is called the *extremal synthesis*. We call the trajectories, that do not depend on the cost[4] J and on the constraints on the control set U, *endpoint singular trajectories* [5]. Endpoint singular trajectories that are also extremals are called *singular extremals*. Extremal trajectories for which $\lambda_0 = 0$ are called *abnormal extremals*. Clearly, abnormal extremals do not depend on the cost J, but depend on the constraint $u \in U$.

[3] A function $f(x)$ satisfies the Lipschitz condition of order α at $x = 0$ if $|f(h) - f(0)| \leq B|h|^\beta$ for all $|h| < \varepsilon$, where B and β are independent of h, $\beta > 0$, and α is an upper bound for all β for which a finite B exists.

[4] For $\bar{\mathcal{H}}(x, \lambda, u) = \lambda . f(x, u)$, solutions to $\dot{x}(t) = \frac{\partial \bar{\mathcal{H}}}{\partial \lambda}$, $\dot{p}(t) = -\frac{\partial \bar{\mathcal{H}}}{\partial x}$ and $\frac{\partial \bar{\mathcal{H}}}{\partial u} = 0$.

[5] i.e., there are singularities in the end-point-mapping $u(.) \to \gamma(T)$ in $[0, T]$

Chapter 5

Mechanics of the Eye Movement: Planer Saccades

The description of right lines and circles, upon which geometry is founded, belongs to mechanics. Geometry does not teach us to draw these lines, but requires them to be drawn.

— Isaac Newton
(*Principia Mathematica.*)

Before discussing the more complex three-dimensional eye movements, let's focus our attention to the movement of the eye on a horizontal plane. The planer movement is controlled by the two muscles, *medial* and *lateral* recti acting as a agonist/antagonist pair. D. A. Robinson (see [Robinson 1964]) is one of the first researchers to propose a mechanical model that could generate planer *saccadic* eye movements resembling to that of humans and monkeys. The model presented here is more detailed in describing the muscle dynamics, compared to the Robinson's original lumped parameter model. This model was first discussed in [Martin & Schovanec 1998] (therefore we call it M-S model) and a study of *smooth pursuit* eye movements using this model is given in [Sugathadasa, Dayawansa & Martin 2000]. As we discussed in Section 2.2, saccades are believed to be happening under open-loop control. In this chapter we propose a "look-up table like" ***learning curves*** to generate the input neural activations.

5.1 Planer model of the eye

The planer eye movements are generated, as we discussed above, due to the action of medial and lateral rectus muscles and a passive moment due to the orbit which restrains the rotation of the globe. Each musculotendon is modeled as a Hill-type complex discussed in Appendix B. Schematic of the model presented here is shown in Figure 5.1 is restricted to horizontal saccadic eye movements. Then the

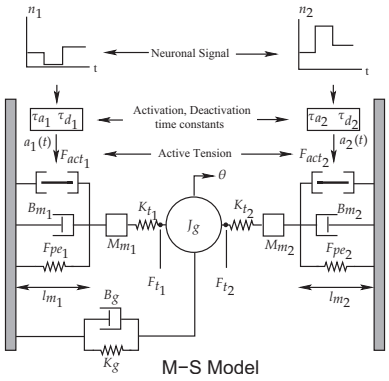

Figure 5.1: The model of the eye plant for horizontal saccades

equation of motion for the eye globe can be written as:

$$J_g\ddot{\theta} + B_g\dot{\theta} + K_g\theta = F_{t_1} - F_{t_2} \tag{5.1}$$

where J_G, B_G, and K_G denote the globe inertia, globe viscosity, and globe elasticity respectively in terms of cgs units and radians. θ is the amount of horizontal rotation and F_{t_1}, F_{t_2} are the forces in the tendons attached to the eye. Note the change in the units where,$J_g = \frac{J_G}{980r(180/\pi)}$ with r denoting the radius of the eye globe. The same applies to B_g, K_g.

In order to represent the model in the form $\dot{x} = f(x) + g_1(x)u_1 + g_2(x)u_2$ where u_1 and u_2 are the neural inputs, let the state vector be

$$x^T(t) = [\theta, \dot{\theta}, l_{m1}, \dot{l}_{m1}, l_{m2}, \dot{l}_{m2}, F_{t_1}, F_{t_2}, a_1, a_2].$$

Then the model can be written as

$$\dot{x} = f(x) + g_1(x)u_1 + g_2(x)u_2$$

where $f(x)$, $g_1(x)$, and $g_2(x)$ can be formulated as follows using equations (B.1), (B.2), (B.4), (B.5), (B.7) as

$$f(x) = \begin{bmatrix} x_2 \\ \frac{1}{J_g}(x_7 - x_8 - B_g x_2 - K_g x_1) \\ x_4 \\ \frac{980}{M}(x_7 - F_{act}(x_3, x_4, x_9) - F_{pe}(x_3) - B_{pm}(\frac{180}{\pi r})x_4) \\ x_6 \\ \frac{980}{M}(x_8 - F_{act}(x_5, x_6, x_{10}) - F_{pe}(x_5) - B_{pm}(\frac{180}{\pi r})x_6) \\ K_t(x_7)\left[-x_2 - (\frac{180}{\pi r})x_4\right] \\ K_t(x_8)\left[x_2 - (\frac{180}{\pi r})x_6\right] \\ -\frac{x_9}{\tau_1} \\ -\frac{x_{10}}{\tau_1} \end{bmatrix}$$

$$g_1(x) = (1/\tau_1)\,[0,0,0,0,0,0,0,0,1,0]$$

$$g_2(x) = (1/\tau_1)\,[0,0,0,0,0,0,0,0,0,1]\,.$$

Typical neural signals, muscle activations, and the resulting saccadic trajectories together with muscle forces are shown in Figures 5.2 and 5.3.

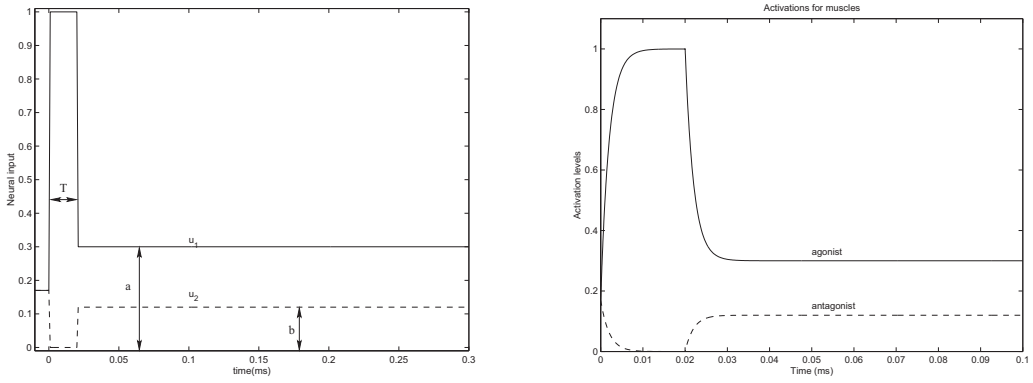

Figure 5.2: Neuronal inputs and the resulting activation signals to the agonist and antagonist (10^0 saccade)

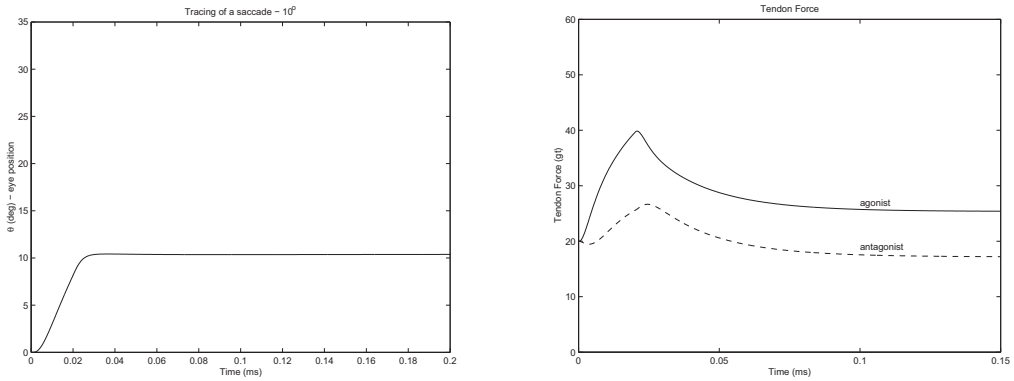

Figure 5.3: Simulation of 10^o Saccade and the corresponding forces in the tendons

5.2 Learning curves

The motorneural signal, shown in Figure 5.2, is composed of a tonic (Step) and a Phasic (Pulse) component. Therefore, the activity curves can be completely parameterized by a, b and T values. Curves which describe the variation of a, b and T for horizontally directed saccades from the primary position are shown in Fig 5.4.

Thus T varies depending on the initial gaze direction and the amplitude of the saccade whereas a and b only depends on the steady state gaze direction. Therefore the parameters (a_1, b_1, T_1) for neuronal activity levels for horizontal saccades originating from any gaze direction can be obtained as

$$\begin{aligned} (a_1, b_1) &= (a_0, b_0) \\ T_1 &= T_0[1 + f_1(\theta_i) g_1(\Delta\theta)] \end{aligned}$$

where θ_i and $\Delta\theta$ are the initial gaze position and saccade amplitude respectively and T_0 corresponds to the T value for a equal amplitude saccade originating from the primary position. $f_1(\theta_i)$ and $g_1(\Delta\theta)$ can be treated as scaling factors.

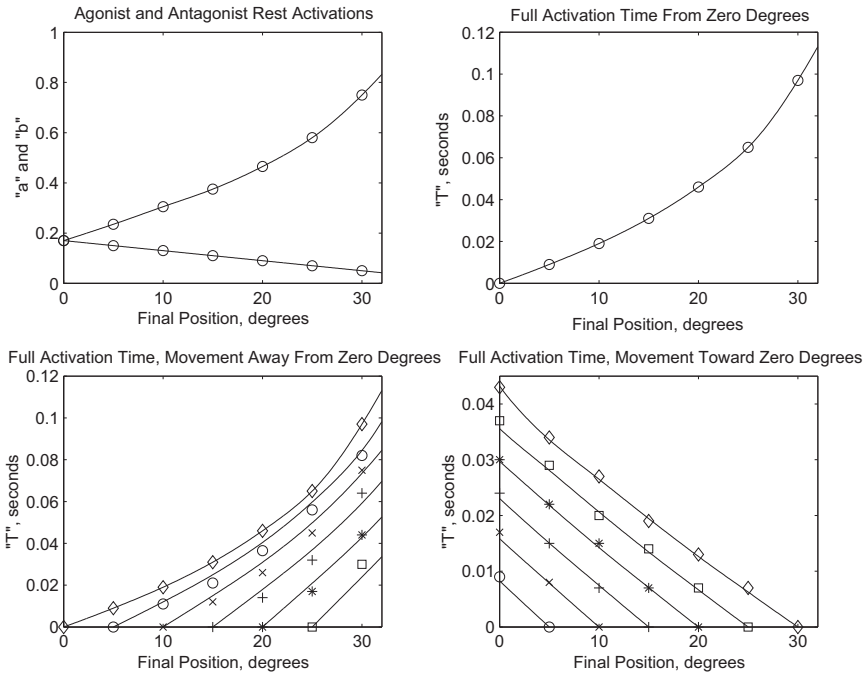

Figure 5.4: "Learning Curves": Cubic Hermite interpolant splines developed from horizontal saccadic eye movements originating from the primary position. The bottom two figures demonstrate how the 'T' value changes with the initial gaze position.

5.3 Remarks

"Learning Curves" enables the control signals (i.e. parameters of neural activity patterns) to be generated rapidly, which is an important issue in fast (< 40ms) saccadic movements. This approach can be compared to the role played by the superior colliculus (SC) leading to a "colliculocentric" model (see [Optican 1994]).

Chapter 6

Mechanics of the Eye Movement: Geometry of Listing Space

The laws of Nature are written in the language of mathematics ... the symbols are triangles, circles and other geometrical figures, without whose help it is impossible to comprehend a single word.

— Galileo Galilei

Human eye, being spherical in shape, has $\mathsf{SO}(3)$, the space of 3×3 rotation matrices, as its natural configuration space. However, from a physiological viewpoint, only the gaze direction vector is important, and the orientation of the eye is otherwise irrelevant. From simple geometric reasoning it follows that each gaze direction of the eye correspond to a circle of rotation matrices in the configuration space. Thus, there is an ambiguity as to which rotation matrix is to be employed to produce a particular gaze direction. Listing's law (see section 2.3) describes precisely how this ambiguity is resolved: all rotation matrices employed have their axes of rotations orthogonal to the standard (or frontal) gaze direction [Tweed & Villis 1990]. Thus, the dynamics of the eye may be treated as a mechanical system with holonomic constraints (see holonomic constraints in section 4.3.2), which in essence limit the configuration space to be a two dimensional submanifold of $\mathsf{SO}(3)$. We will refer to it as the ***Listing Space***. In this Chapter we will describe basic geometric features of the Listing Space. This then will enable one to formulate

dynamic equations of the eye motion using various neuro/muscular models and we will discuss them in the next Chapter.

We make the following fundamental assumptions throughout:

- Eye is a perfect sphere.
- All eye movements obey Listings law.

We remark here that the second assumption pertains to all eye configurations throughout its motions, and not just on the initial and final points of an eye movement.

6.1 Listing Manifold is Diffeomorphic to the Projective Space

Listings law states that all eye rotations have an axis orthogonal to the primary gaze direction. If we were to take the (x_1, x_2, x_3) axes such that x_3 axis is aligned with the normal gaze direction, then Listing's law amounts to a statement that all eye rotations have quaternion representations $q \in S^3$ with $q_3 = 0$. We denote by ***List***, the subset of $\mathsf{SO}(3)$ which obey Listing's law. In this section we will show that ***List*** is diffeomorphic to the projective space $\mathbb{P}^2$.

Let us consider the map,

$$\begin{aligned} \mathbf{emb} \quad : \quad & \mathbb{R}^3 \to S^3, \\ & (x_1, x_2, x_3) \mapsto \frac{1}{\sqrt{1 + ||x||^2}} \begin{bmatrix} 1 \\ x_1 \\ x_2 \\ x_3 \end{bmatrix}. \end{aligned}$$

Let us observe that $\mathbf{emb}(x)$ is the quaternion which describes a rotation around $(1/||x||)x$ by an angle $2arctan(||x||)$ (where the angle is in $[0, \pi)$). The ambiguity at $x = 0$ is resolved by mapping it to $\overrightarrow{\mathbf{1}}$. Therefore, each vector with zero x_3 coordinate describes a unique Listing rotation. However, those Listing rotations with angle of rotation equal to π are missing here. Let us observe that a rotation by π around an axis n is identical to a rotation by an angle $-\pi$ around $-n$. Thus we may describe ***List*** by appropriately compactifying $\mathbb{R}^3$. This compactification

is best understood in the following way. Let us start with $\mathbb{R}^4$ with coordinates (x_0, x_1, x_2, x_3) and put the usual projective equivalence relation that collapse one dimensional subspaces to points. This way, each $(x_1, x_2, x_3) \in \mathbb{R}^3$ is identified with the equivalence class of $(1, x_1, x_2, x_3)$, hence associated with the unique rotation of $\mathbf{emb}(x_1, x_2, x_3)$. Equivalence classes of $(0, x_1, x_2, x_3)$ are uniquely associated with rotations by an angle of π or $-\pi$. This association is unambiguous since rotation by π and $-\pi$ around the unit vector n amounts to the same rotation matrix in $\mathsf{SO}(3)$. Thus we conclude that the space ***List*** is diffeomorphic to $\mathbb{P}^2$.

This identification provides an obvious way to come up with local coordinates on ***List***. However, it turns that the description of a natural Riemannian metric on ***List*** is quite awkward using these coordinates. Hence, we will use an axis-angle local coordinate system to carry out most of our computation. The two local coordinates (θ, ϕ) describe the polar coordinate angle of the axis of rotation in the (x_1, x_2) plane and the angle of rotation around the axis respectively. Here we take $(\theta, \phi) \in [0, \pi] \times [0, 2\pi]$. Of course we must keep in mind that these fail to be local coordinates when $\phi = 0$ or $\phi = 2\pi$ since in these cases the corresponding rotation is the identity regardless of the value of θ.

6.2 Riemannian Metric on *List*

Let us assume that the eye is a perfect sphere, and its moment of inertia is equal to $\mathbb{I}_{3\times3}$. This is associated with the left invariant Riemannian metric on $\mathsf{SO}(3)$ given by,

$$\left\langle \mathbf{\Omega}(e_i), \mathbf{\Omega}(e_j) \right\rangle_I = \delta_{i,j},$$

where,

$$\mathbf{\Omega}(e_k) = \begin{bmatrix} 0 & \delta_{3,k} & -\delta_{2,k} \\ -\delta_{3,k} & 0 & \delta_{1,k} \\ \delta_{2,k} & -\delta_{1,k} & 0 \end{bmatrix},$$

and $\{\delta_{l,m}\}$ denotes the Kronecker delta function. An easy way to carry out computation using this Riemannian metric is provided by the isometric submersion **rot**.

Notice that $\vec{\mathbf{i}}, \vec{\mathbf{j}}, \vec{\mathbf{k}}$ is an orthonormal basis of $\mathsf{T}_{\vec{1}}S^3$, and

$$\mathbf{rot}\left(\begin{bmatrix}\cos(t/2)\\ \sin(t/2)\\ 0\\ 0\end{bmatrix}\right) = e^{t\mathbf{\Omega}(e_1)}, \qquad \mathbf{rot}\left(\begin{bmatrix}\cos(t/2)\\ 0\\ \sin(t/2)\\ 0\end{bmatrix}\right) = e^{t\mathbf{\Omega}(e_2)},$$

$$\mathbf{rot}\left(\begin{bmatrix}\cos(t/2)\\ 0\\ 0\\ \sin(t/2)\end{bmatrix}\right) = e^{t\mathbf{\Omega}(e_3)}.$$

Hence, it follows that $\mathbf{rot}_{*\vec{1}}\vec{\mathbf{i}} = 2\mathbf{\Omega}(e_1)$, $\mathbf{rot}_{*\vec{1}}\vec{\mathbf{j}} = 2\mathbf{\Omega}(e_2)$ and $\mathbf{rot}_{*\vec{1}}\vec{\mathbf{k}} = 2\mathbf{\Omega}(e_3)$, hence $\{\mathbf{rot}_{*\vec{1}}\vec{\mathbf{i}}/2,\ \mathbf{rot}_{*\vec{1}}\vec{\mathbf{j}}/2, \mathbf{rot}_{*\vec{1}}\vec{\mathbf{k}}/2\}$ is an orthonormal frame in $\mathsf{T}_{\mathrm{Id}}(\mathsf{SO}(3))$ (see equations (4.4) and (4.5) in section 4.2.1). Now, since **rot** is equivariant under left translations, and Riemannian metrics on S^3 as well as on $\mathsf{SO}(3)$ are left invariant, it follows that $\{\mathbf{rot}_{*q}\vec{\mathbf{i}}/2, \mathbf{rot}_{*q}\vec{\mathbf{j}}/2, \mathbf{rot}_{*q}\vec{\mathbf{k}}/2\}$ is an orthonormal basis of $\mathsf{T}_{\mathbf{rot}(q)}\mathsf{SO}(3)$ for all $q \in S^3$.

$$\begin{array}{ccc} S^3 & \xrightarrow{\mathbf{rot}} & \mathsf{SO}(3) \\ \downarrow & & \downarrow \\ \mathsf{T}_qS^3 & \xrightarrow{\mathbf{rot}_*} & \mathsf{T}_{\mathbf{rot}(q)}\mathsf{SO}(3) \end{array}$$

Let us now use the orthonormal frame $\{q.\vec{\mathbf{i}}/2, q.\vec{\mathbf{j}}/2, q.\vec{\mathbf{k}}/2\}$ of T_qS^3 to compute the Riemannian metric on ***List*** induced from $\mathsf{SO}(3)$ (see induced metric, in proposition 3.2.1).

Let us define,

$$\begin{aligned} g_{11} &= \left\langle \frac{\partial}{\partial\theta}, \frac{\partial}{\partial\theta} \right\rangle \\ g_{12} &= \left\langle \frac{\partial}{\partial\theta}, \frac{\partial}{\partial\phi} \right\rangle \\ g_{22} &= \left\langle \frac{\partial}{\partial\phi}, \frac{\partial}{\partial\phi} \right\rangle. \end{aligned} \tag{6.1}$$

Let $\rho : [0, \pi] \times [0, 2\pi] \to S^3$,

$$\rho(\theta, \phi) = \begin{bmatrix} \cos(\phi/2) \\ cos(\theta)sin(\phi/2) \\ sin(\theta)sin(\phi/2) \\ 0 \end{bmatrix}.$$

This can be illustrated as follows:

$$\begin{array}{ccc} \textbf{\textit{List}} & \xrightarrow{\rho} & S^3 \\ \downarrow & & \downarrow \\ \mathsf{T}_{(\theta,\phi)}\textbf{\textit{List}} & \xrightarrow{\rho_*} & \mathsf{T}_{\rho(\theta,\phi)}S^3 \end{array}$$

Then

$$\mathcal{J}(\rho)(\theta, \phi) = \begin{pmatrix} \rho_*(\frac{\partial}{\partial\theta}) & \rho_*(\frac{\partial}{\partial\phi}) \end{pmatrix} = \begin{pmatrix} 0 & -\frac{1}{2}sin(\phi/2) \\ -sin(\theta)sin(\phi/2) & \frac{1}{2}cos(\theta)cos(\phi/2) \\ cos(\theta)sin(\phi/2) & \frac{1}{2}sin(\theta)cos(\phi/2) \\ 0 & 0 \end{pmatrix}$$

Notice that

$$\rho(\theta, \phi).\vec{\mathbf{i}} = \begin{bmatrix} -cos(\theta)sin(\phi/2) \\ cos(\phi/2) \\ 0 \\ -sin(\theta)sin(phi/2) \end{bmatrix}, \qquad \rho(\theta, \phi).\vec{\mathbf{j}} = \begin{bmatrix} -sin(\theta)sin(\phi/2) \\ 0 \\ cos(\phi/2) \\ cos(\theta)sin(\phi/2) \end{bmatrix},$$

$$\rho(\theta, \phi).\vec{\mathbf{k}} = \begin{bmatrix} 0 \\ sin(\theta)sin(\phi/2) \\ -cos(\theta)sin(\phi/2) \\ cos(\phi/2) \end{bmatrix}.$$

Then, for $\theta = 0$, it is easily observed that,

$$\begin{aligned} \rho_{*(0,\phi)}(\frac{\partial}{\partial\theta}) &= sin(\phi/2)cos(\phi/2)\rho(0, \phi).\vec{\mathbf{j}} - sin^2(\phi/2)\rho(0, \phi).\vec{\mathbf{k}}, \\ \rho_{*(0,\phi)}(\frac{\partial}{\partial\phi}) &= \frac{1}{2}\rho(0, \phi).\vec{\mathbf{i}}. \end{aligned}$$

Hence according to Proposition 3.2.1, we have,

$$\langle u, v\rangle_{\textbf{\textit{List}}} = \left\langle \rho_{*(0,\phi)}(u), \rho_{*(0,\phi)}(v)\right\rangle_{S^3}, \qquad u, v \in \mathsf{T}_{(0,\phi)}\textbf{\textit{List}}.$$

Therefore using the relations given in equation (6.1) and proper scaling

$$\begin{aligned} g_{11} &= 4sin^2(\phi/2), \\ g_{12} &= 0, \\ g_{22} &= 1. \end{aligned}$$

Thus, the Riemannian metric on ***List***, using the result in equation (3.8), is,

$$g = 4sin^2(\phi/2)d\theta^2 + d\phi^2.$$

Notice that this expression is singular at $\phi = 0$. This represents the fact that (θ, ϕ) fail to be local coordinates around $\phi = 0$.

6.3 Geometry of the Listing Space

6.3.1 Connection on *List*

Let us compute the Riemannian connection, ∇, on ***List*** now. It is well known that ∇ is uniquely defined by the formula (see Section 3.6 and [Boothby 1986]),

$$\begin{aligned} 2\langle \nabla_X Y, Z\rangle &= \mathscr{L}_X\langle Y, Z\rangle + \mathscr{L}_Y\langle X, Z\rangle - \mathscr{L}_Z\langle X, Y\rangle \\ &\quad -\langle X, [Y, Z]\rangle - \langle Y, [X, Z]\rangle + \langle Z, [X, Y]\rangle \end{aligned} \tag{6.2}$$

Let us use subscripted coordinates (y_1, y_2) to denote (θ, ϕ). Then,∇ can be described in local coordinates (y_1, y_2) via,

$$\nabla_{\partial y_i/\partial y_j} = \Gamma_{ij}^k \partial/\partial y_k,$$

where, $\Gamma^k_{i,j}$ are the Christoffel symbols [do Carmo 1993]. They can be calculated using Equation (3.12):

$$\Gamma^k_{ij} = \sum_{h=1}^{2} \frac{g^{ih}}{2} \left\{ \frac{\partial g_{hj}}{\partial y_k} + \frac{\partial g_{hk}}{\partial y_j} - \frac{\partial g_{jk}}{\partial y_h} \right\} \quad i, j, k = 1, 2$$

and the symmetry property given in Equation (3.11). Here

$$(g_{ij}) = \begin{pmatrix} g_{11} & g_{12} \\ g_{21} & g_{22} \end{pmatrix} = \begin{pmatrix} 4\sin^2(\phi/2) & 0 \\ 0 & 1 \end{pmatrix}, \qquad \text{(lower } g\text{-}ij\text{'s)}$$

and,

$$(g^{ij}) = \begin{pmatrix} g^{11} & g^{12} \\ g^{21} & g^{22} \end{pmatrix} = \begin{pmatrix} \frac{1}{4\sin^2(\phi/2)} & 0 \\ 0 & 1 \end{pmatrix}. \qquad \text{(upper } g\text{-}ij\text{'s)}$$

Thus, we obtain expressions for Christoffel symbols,

$$\begin{aligned} \Gamma^1_{11} &= 0, & \Gamma^2_{11} &= -sin(\phi), \\ \Gamma^1_{12} &= \frac{1}{2tan(\phi/2)}, & \Gamma^1_{21} &= \frac{1}{2tan(\phi/2)}, \\ \Gamma^2_{12} &= 0, & \Gamma^2_{21} &= 0, \\ \Gamma^1_{22} &= 0, & \Gamma^2_{22} &= 0. \end{aligned}$$

6.3.2 Equations of Geodesics on *List*

Christoffel symbols can be used to compute parallel transport on ***List***. In particular, one may derive equations for geodesics (see section 3.2.3) using them. Let $\sigma(t) = (\theta(t), \phi(t))$ be a geodesic on ***List***. Then from Equation (3.5), we have,

$$\nabla_{\dot\sigma(t)} \dot\sigma(t) = 0,$$

where

$$\dot\sigma(t) = \left(\dot\theta \frac{\partial}{\partial\theta} + \dot\phi \frac{\partial}{\partial\phi} \right)$$

Now,

$$\begin{aligned}
\nabla_{\dot\sigma(t)}\dot\sigma(t) &= \nabla_{\left(\dot\theta\frac{\partial}{\partial\theta}+\dot\phi\frac{\partial}{\partial\phi}\right)}\left(\dot\theta\frac{\partial}{\partial\theta}+\dot\phi\frac{\partial}{\partial\phi}\right)\\
&= \left(\dot\theta\nabla_{\frac{\partial}{\partial\theta}}+\dot\phi\nabla_{\frac{\partial}{\partial\phi}}\right)\left(\dot\theta\frac{\partial}{\partial\theta}+\dot\phi\frac{\partial}{\partial\phi}\right) \qquad \text{(Using (3.7a))}\\
&= \dot\theta\nabla_{\frac{\partial}{\partial\theta}}\left(\dot\theta\frac{\partial}{\partial\theta}\right)+\dot\theta\nabla_{\frac{\partial}{\partial\theta}}\left(\dot\phi\frac{\partial}{\partial\phi}\right)\\
&\qquad +\dot\phi\nabla_{\frac{\partial}{\partial\phi}}\left(\dot\theta\frac{\partial}{\partial\theta}\right)+\dot\phi\nabla_{\frac{\partial}{\partial\phi}}\left(\dot\phi\frac{\partial}{\partial\phi}\right) \qquad \text{(Using (3.7b))}\\
&= \ddot\theta\frac{\partial}{\partial\theta}+\ddot\phi\frac{\partial}{\partial\phi}+\dot\theta^2\nabla_{\frac{\partial}{\partial\theta}}\frac{\partial}{\partial\theta}\\
&\qquad +\dot\theta\dot\phi(\nabla_{\frac{\partial}{\partial\theta}}\frac{\partial}{\partial\phi}+\nabla_{\frac{\partial}{\partial\phi}}\frac{\partial}{\partial\theta})+\dot\phi^2\nabla_{\frac{\partial}{\partial\phi}}\frac{\partial}{\partial\phi}. \qquad \text{(Using (3.7c))}
\end{aligned}$$

Hence,

$$\ddot\theta\frac{\partial}{\partial\theta}+\ddot\phi\frac{\partial}{\partial\phi}+\dot\theta^2\nabla_{\frac{\partial}{\partial\theta}}\frac{\partial}{\partial\theta}+\dot\theta\dot\phi(\nabla_{\frac{\partial}{\partial\theta}}\frac{\partial}{\partial\phi}+\nabla_{\frac{\partial}{\partial\phi}}\frac{\partial}{\partial\theta})+\dot\phi^2\nabla_{\frac{\partial}{\partial\phi}}\frac{\partial}{\partial\phi}=0.$$

Using

$$\begin{aligned}
\nabla_{\frac{\partial}{\partial\theta}}\frac{\partial}{\partial\theta}&=\sum_{k=1}^{2}\Gamma^k_{11}\frac{\partial}{\partial y_k}=-\sin(\phi)\frac{\partial}{\partial\phi}, \qquad \nabla_{\frac{\partial}{\partial\theta}}\frac{\partial}{\partial\phi}=\sum_{k=1}^{2}\Gamma^k_{12}\frac{\partial}{\partial y_k}=\frac{1}{2\tan(\phi/2)}\frac{\partial}{\partial\theta},\\
\nabla_{\frac{\partial}{\partial\phi}}\frac{\partial}{\partial\theta}&=\sum_{k=1}^{2}\Gamma^k_{21}\frac{\partial}{\partial y_k}=\frac{1}{2\tan(\phi/2)}\frac{\partial}{\partial\theta}, \quad \nabla_{\frac{\partial}{\partial\phi}}\frac{\partial}{\partial\phi}=\sum_{k=1}^{2}\Gamma^k_{22}\frac{\partial}{\partial y_k}=0,
\end{aligned}$$

where $(y_1, y_2) = (\theta, \phi)$, we obtain the equations of geodesics,

$$\begin{aligned}
\ddot\theta+\frac{1}{tan(\phi/2)}\dot\theta\dot\phi&=0,\\
\ddot\phi-sin\phi\dot\theta^2&=0.
\end{aligned} \tag{6.3}$$

Figure 6.1 display geodesics emanating from $(\pi/4, \pi/4)$ in the Listing space.

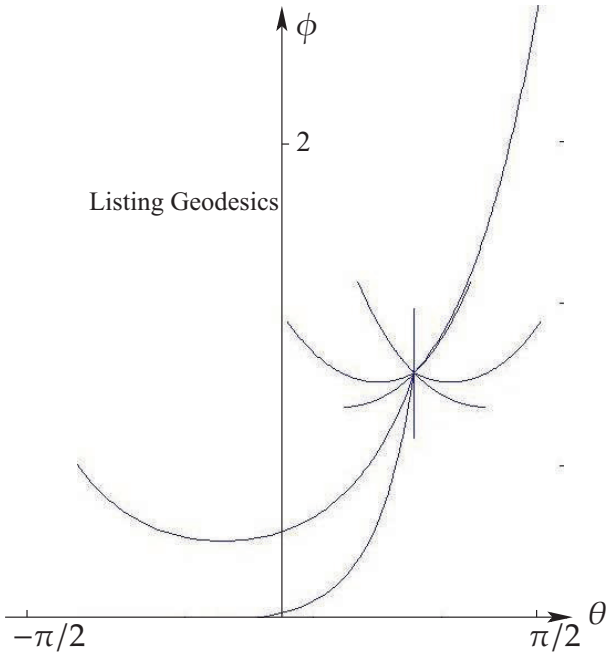

Figure 6.1: Geodesics emanating from$(\pi/4, \pi/4)$

6.3.3 Curvature

From the Christoffel symbols we may compute the Riemann curvature tensor $\mathcal{R}$ using the Definition 3.16. In terms of the basis[1] $\{\partial_\theta, \partial_\phi\}$, Equation (3.13) becomes

$$\mathcal{R}(\partial_\theta, \partial_\phi)\partial_\theta = \nabla_{\partial_\theta}\nabla_{\partial_\phi}\partial_\theta - \nabla_{\partial_\phi}\nabla_{\partial_\theta}\partial_\theta, \qquad \text{since } [\partial_\theta, \partial_\phi] = 0,$$

this evaluates to,

$$\begin{aligned} \mathcal{R}(\partial_\theta, \partial_\phi)\partial_\theta &= -cos(\phi/2)\partial_\theta \\ \mathcal{R}(\partial_\theta, \partial_\phi)\partial_\phi &= \frac{1}{4}\partial_\theta. \end{aligned}$$

In particular, the Gauss curvature is given by,

$$\begin{aligned} K(\theta, \phi) &= \left\langle \mathcal{R}(\partial_\theta, \partial_\phi)\partial_\phi, \partial_\theta \right\rangle / \langle \partial_\theta, \partial_\theta \rangle \\ &= 1/4 \end{aligned}$$

The fact that the Gauss curvature is constant, is indeed very surprising.

[1] We use the short notation $\partial_\theta = \frac{\partial}{\partial\theta}$

Chapter 7

Mechanics of the Eye Movement: Optimal Control

I can tell the lion by its claws

— Johann Bernoulli
(After reading an anonymous solution to the Brachystochrone problem that he realized was Newton's solution.)

In this chapter, we will discuss how the results presented in Chapter 4 can be applied in the eye movement control. Lagrangian and Hamiltonian formulations are presented together with an application of the Maximum principle in order to obtain optimal trajectories minimizing the control energy. We will compare these trajectories with geodesics on ***List*** and SO(3) trajectories. Finally, the application of a neuro/muscular models is discussed.

7.1 Equations of motion

Let us write down a potential function in the form $V(\theta, \phi)$ and generalized forces τ_θ, τ_ϕ. Now the Lagrangian (see section 4.3.1) is,

$$L(\theta, \phi, \dot{\theta}, \dot{\phi}) = \frac{1}{2}\|\dot{\theta}\frac{\partial}{\partial\theta} + \dot{\phi}\frac{\partial}{\partial\phi}\|^2 - V(\theta, \phi). \tag{7.1}$$

Hence, from Euler-Lagrange equations given in equation (4.13) , we obtain equations of motion,

$$\begin{aligned} \ddot{\theta} + \dot{\theta}\dot{\phi}cot(\phi/2) + \frac{1}{4}csc^2(\phi/2)\frac{\partial}{\partial\theta}V &= \frac{1}{4}csc^2(\phi/2)\tau_\theta \\ \ddot{\phi} - \dot{\theta}^2\sin(\phi) + \frac{\partial}{\partial\phi}V &= \tau_\phi. \end{aligned} \tag{7.2}$$

Notice that when $V(\theta, \phi) = 0$, i.e., the Lagrangian becomes only the kinetic energy, and no forces acting on the system, Equation (7.2) reduces to that of geodesics given in Equation (6.3).

7.2 Optimal control

7.2.1 Case I: Generalized torques

Let us take $V(\theta, \phi) = sin^2(\phi/2)$. Equations (7.2) become

$$\begin{aligned} \ddot{\theta} + \dot{\theta}\dot{\phi}\cot(\phi/2) &= \frac{1}{4}csc^2(\phi/2)\tau_\theta \\ \ddot{\phi} - \dot{\theta}^2\sin(\phi) + \frac{1}{2}\sin(\phi) &= \tau_\phi. \end{aligned} \tag{7.3}$$

Let $[z_1, z_2, z_3, z_4]' = [\theta, \dot{\theta}, \phi, \dot{\phi}]'$, then (7.3) can be written as

$$\frac{d}{dt}\begin{bmatrix} z_1 \\ z_2 \\ z_3 \\ z_4 \end{bmatrix} = \begin{bmatrix} z_2 \\ -z_2 z_4 cot(z_3/2) \\ z_4 \\ z_2^2 sin(z_3) - \frac{1}{2}sin(z_3) \end{bmatrix} + \begin{bmatrix} 0 \\ \frac{1}{4}csc^2(z_3/2) \\ 0 \\ 0 \end{bmatrix}\tau_\theta + \begin{bmatrix} 0 \\ 0 \\ 0 \\ 1 \end{bmatrix}\tau_\phi \tag{7.4}$$

Assume that we wish to control the state $(\theta, \dot{\theta}, \phi, \dot{\phi})$ from $(\theta_0, 0, \phi_0, 0)$ to $(\theta_1, 0, \phi_1, 0)$ in T unit of time, while minimizing the control energy,

$$\int_0^T \left[(\tau_\theta(t))^2 + (\tau_\phi(t))^2\right] \mathrm{d}t.$$

Let the Lagrangian be

$$L = \frac{1}{2}\left((\tau_\theta(t))^2 + (\tau_\phi(t))^2\right),$$

and denote the costate by λ. Construct the Hamiltonian

$$\begin{aligned}\mathcal{H}(z,\lambda) &= \lambda.\dot{z} - L(z)\\ &= \lambda_1 z_2 - \lambda_2 z_2 z_4 \cot(z_3/2) + \lambda_3 z_4 + \lambda_4 z_2^2 \sin(z_3) - \frac{1}{2}\lambda_4 \sin(z_3)\\ &\qquad \frac{\lambda_2}{4\sin^2(z_3/2)}\tau_\theta + c\lambda_4\tau_\phi + \frac{1}{2}\left((\tau_\theta(t))^2 + (\tau_\phi(t))^2\right)\end{aligned}$$

Then the Hamiltonian system (using the Equations (4.16)) becomes

$$\frac{d}{dt}\begin{bmatrix} z_1\\ z_2\\ z_3\\ z_4\\ \lambda_1\\ \lambda_2\\ \lambda_3\\ \lambda_4\end{bmatrix} = \begin{bmatrix} z_2\\ -z_2 z_4 cot(z_3/2) + 1/4 sin^2(z_3/2)\tau_\theta^*\\ z_4\\ z_2^2 sin(z_3) - \frac{1}{2}sin(z_3) + \tau_\phi^*\\ 0\\ -\lambda_1 + \lambda_2 z_4 cot(z_3/2) - 2\lambda_4 z_2 sin(z_3)\\ -\frac{1}{2}\lambda_2 z_2 z_4 csc^2(z_3/2) - \lambda_4 z_2^2 cos z_3 + \frac{1}{2}\lambda_4 cos(z_3) + \frac{1}{2}\lambda_2 cot(z_3) csc^2(z_3)\tau_\theta^*\\ \lambda_2 z_2 cot(z_3/2) - \lambda_3\end{bmatrix}$$

According to the Maximum Principle (see Section 4.4), one can obtain the following controls

$$\begin{aligned}\tau_\theta &= -\frac{\lambda_2}{4\sin^2(z_3/2)},\\ \tau_\phi &= -\lambda_4.\end{aligned}$$

Therefore, the system becomes,

$$\begin{bmatrix} \dot{z}_1 \\ \dot{z}_2 \\ \dot{z}_3 \\ \dot{z}_4 \\ \dot{\lambda}_1 \\ \dot{\lambda}_2 \\ \dot{\lambda}_3 \\ \dot{\lambda}_4 \end{bmatrix} = \begin{bmatrix} z_2 \\ -z_2 z_4 cot(z_3/2) - \frac{\lambda_2}{16} csc^4(z_3/2) \\ z_4 \\ z_2^2 sin(z_3) - \frac{1}{2} sin(z_3) - \lambda_4 \\ 0 \\ -\lambda_1 + \lambda_2 z_4 cot(z_3/2) - 2\lambda_4 z_2 sin(z_3) \\ (-\frac{1}{2}\lambda_2 z_2 z_4 csc^2(z_3/2) - \lambda_4 z_2^2 cos(z_3) + \\ \frac{1}{2}\lambda_4 cos(z_3/2) - \frac{\lambda_2^2}{16} csc^4(z_3/2) cot(z_3/2)) \\ \lambda_2 z_2 cot(z_3/2) - \lambda_3 \end{bmatrix}. \tag{7.5}$$

Figure 7.1(a) shows an example of an optimal path in the Listing space and Figure 7.2(b) shows the corresponding torques.

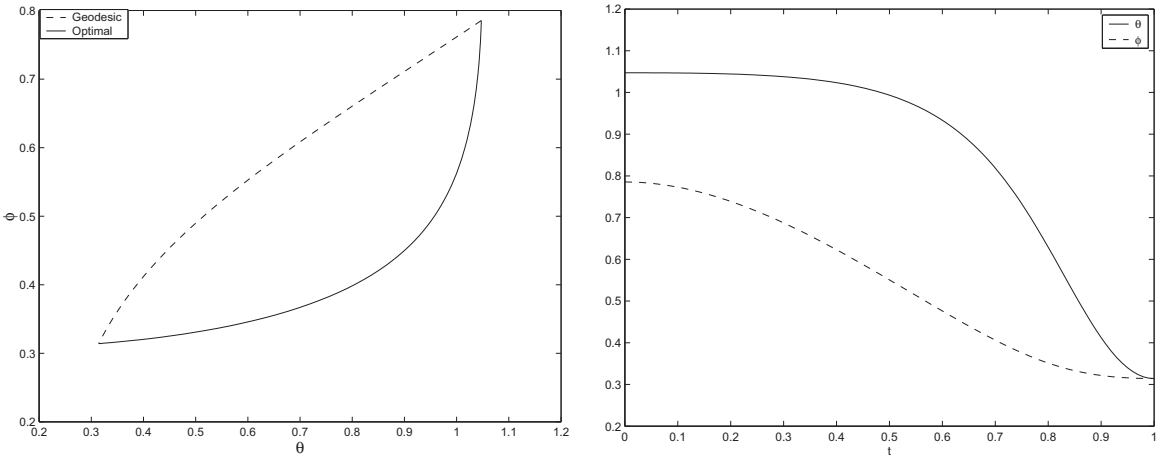

(a) Optimal path and the geodesic (θ, ϕ)

(b) θ and ϕ with time

Figure 7.1: Optimal path from $(\pi/3, \pi/4)$ to $(\pi/10, \pi/10)$ for Case I

7.2.2 Case II: Simplified muscles

Here we assume a linearized model for each of the six musculotendons. Let each musculotendon consist of a linear spring with spring constant k_i, a damper with damping constant b_i, and an active force F_i, where $i = 1 \ldots 6$.

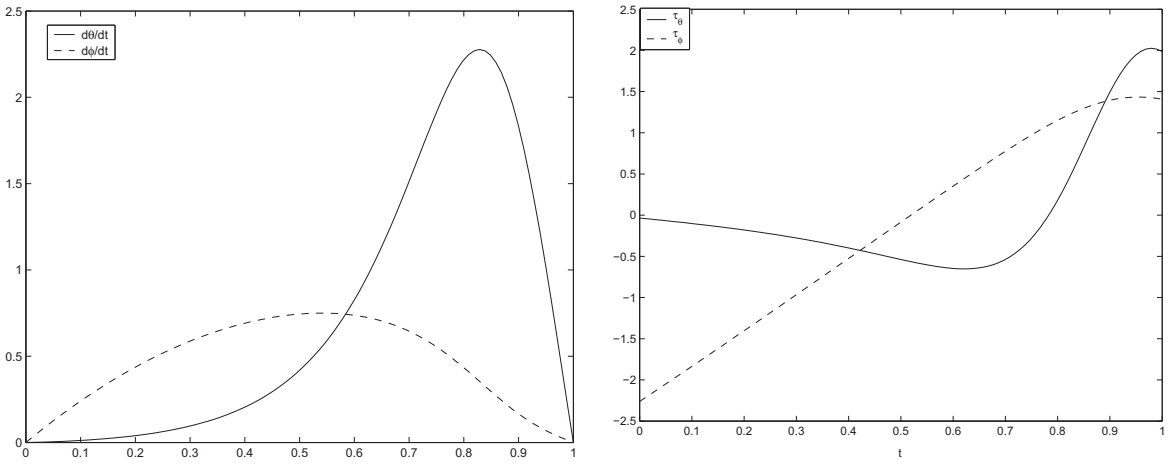

(a) $\dot{\theta}, \dot{\phi}$ (b) τ_θ and τ_ϕ for the optimal path

Figure 7.2: $\dot{\theta}, \dot{\phi}$ and τ_θ, τ_ϕ corresponding to Optimal path from $(\pi/3, \pi/4)$ to $(\pi/10, \pi/10)$ for Case I

Projecting the torques to *List*

Assume the changes in θ and ϕ as $\theta \longrightarrow \theta + \delta\theta$ and $\phi \longrightarrow \phi$.
Virtual work by the spring: $k_i(l_i - l_{i_0})\delta l = k_i(l_i - l_{i_0})\frac{\partial l_i}{\partial \theta} d\theta$. Thus

$$\tau_\theta = k_i(l_i - l_{i_0})\frac{\partial l_i}{\partial \theta}.$$

Also note,

$$\dot{l}_i = \dot{\theta}\frac{\partial l_i}{\partial \theta} + \dot{\phi}\frac{\partial l_i}{\partial \phi}.$$

Therefore for the damper:

$$F_{damp} = b_i\dot{l}_i = b_i(\dot{\theta}\frac{\partial l_i}{\partial \theta} + \dot{\phi}\frac{\partial l_i}{\partial \phi})$$

Then the torque with the active force F_i

$$\begin{aligned} \tau_\theta &= \sum_{i=1}^{6} [F_i + C_i] \frac{\partial l_i}{\partial \theta} \\ \tau_\phi &= \sum_{i=1}^{6} [F_i + C_i] \frac{\partial l_i}{\partial \phi} \end{aligned} \tag{7.6}$$

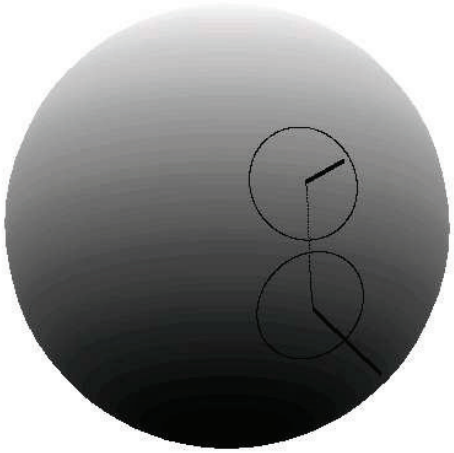

Figure 7.3: Optimal path in R^3 for Case I

where

$$C_i = k_i(l_i - l_{i_0}) + b_i(\dot{\theta}\frac{\partial l_i}{\partial \theta} + \dot{\phi}\frac{\partial l_i}{\partial \phi}). \tag{7.7}$$

Now the optimal control problem becomes one of minimizing

$$\int_0^T \sum_{i=1}^{6} F_i^2 \mathrm{d}t. \tag{7.8}$$

Therefore, let $L = \frac{1}{2}\sum_{i=1}^{6} F_i^2$ and construct the Hamiltonian

$$\begin{aligned}\mathcal{H}(z,\lambda) &= \lambda_1 z_2 - \lambda_2 z_2 z_4 cot(z_3/2) + \lambda_3 z_4 + \lambda_4 z_2^2 sin(z_3) - \frac{1}{2}\lambda_4 sin(z_3) + \\ &\quad \frac{\lambda_2}{4sin(z_3/2)}\sum_{i=1}^{6}[F_i + C_i]\frac{\partial l_i}{\partial \theta} + \lambda_4 \sum_{i=1}^{6}[F_i + C_i]\frac{\partial l_i}{\partial \phi} + L(z).\end{aligned}$$

Maximum principle gives

$$F_i^* = -\frac{\lambda_2}{4sin^2(z_3/2)}\frac{\partial l_i}{\partial \theta} - \lambda_4 \frac{\partial l_i}{\partial \phi}$$

Hence

$$\tau_\theta^* = \sum_{i=1}^{6}\left\{-\frac{\lambda_2}{4sin^2(z_3/2)}\frac{\partial l_i}{\partial \theta} - \lambda_4\frac{\partial l_i}{\partial \phi} + C_i\right\}\frac{\partial l_i}{\partial \theta}$$

$$\tau^*_\phi = \sum_{i=1}^{6} \left\{ -\frac{\lambda_2}{4sin^2(z_3/2)} \frac{\partial l_i}{\partial \theta} - \lambda_4 \frac{\partial l_i}{\partial \phi} + C_i \right\} \frac{\partial l_i}{\partial \phi}$$

Let's find $\frac{\partial l_i}{\partial \theta}$ and $\frac{\partial l_i}{\partial \phi}$:
Let q_i and $p_i(t)$ be the fixed end and the point of attachment to the eye, of the muscle. Then,

$$l_i^2(t) = (p_i(t) - q_i)^T (p_i(t) - q_i)$$

where $p_i(t) = \boldsymbol{R} p_i(0)$ and $\boldsymbol{R}$ is the 3×3 rotation matrix.
Then

$$\begin{aligned} l_i^2(t) &= (\boldsymbol{R} p_i(0) - q_i)^T (\boldsymbol{R} p_i(0) - q_i) \\ &= p_i^T(0) p_i(0) + q_i q_i^T - 2 p_i^T(0) \boldsymbol{R}^T q_i \end{aligned} \tag{7.9}$$

Therefore

$$\begin{aligned} \frac{\partial l_i}{\partial \theta} &= -p_i^T(0) \left(\frac{\partial \boldsymbol{R}^T}{\partial \theta} \right) q_i / l_i \\ \frac{\partial l_i}{\partial \phi} &= -p_i^T(0) \left(\frac{\partial \boldsymbol{R}^T}{\partial \phi} \right) q_i / l_i. \end{aligned} \tag{7.10}$$

Then one can write down the system with state z and costate λ similar to the one given in Equation (7.5). Figure 7.5 shows the optimal path and the corresponding rectus muscle forces.

7.2.3 Case III: Hill-type muscles

Hill-type muscle model is described in detail in Appendix B. Formulation follows very closely to that of given in Section 7.2.2. Here

$$\begin{aligned} \tau_\theta &= \sum_{i=1}^{6} F^i_{\text{total}} \frac{\partial l_i}{\partial \theta} \\ \tau_\phi &= \sum_{i=1}^{6} F^i_{\text{total}} \frac{\partial l_i}{\partial \phi} \end{aligned} \tag{7.11}$$

where

$$F^i_{\text{total}} = F^i_t - (F^i_{act} + F^i_{pe} + B^i_m \dot{l}_i).$$

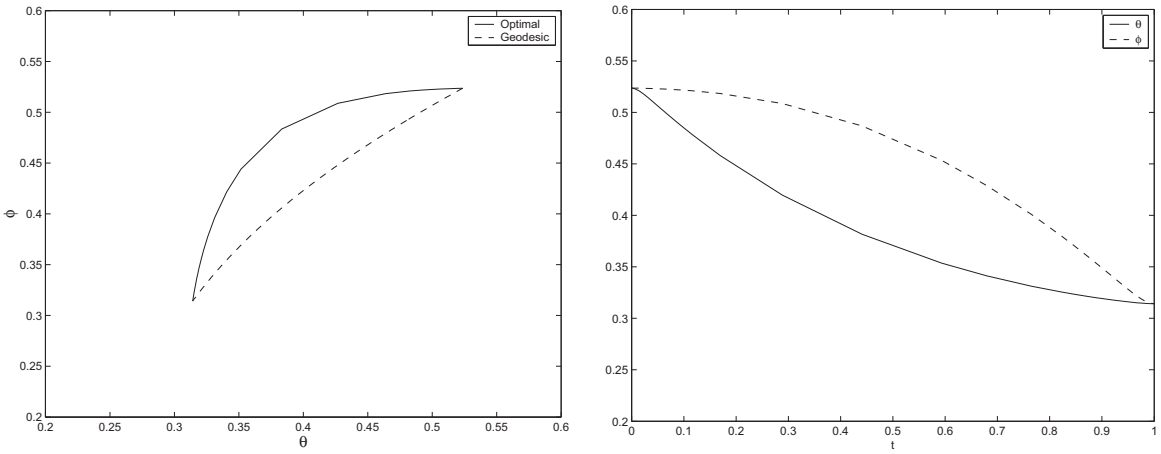

(a) Optimal path and the geodesic (θ, ϕ) (b) θ and ϕ with time

Figure 7.4: Optimal path from $(\pi/6, \pi/6)$ to $(\pi/10, \pi/10)$ for Case II

The terms $F_t, F_{act}, F_{pe}, B_m$ above are described in Appendix B and i indexes each muscle.

According to Equation (B.2), without loosing any generality, one could minimize the active force in the muscle $F_{act}(t)$ instead of minimizing the activation $a(t)$. Therefore the problem beomes one of minimizing

$$\int_0^T \sum_{i=1}^{6} [F_{act}(t)]^2 \, \mathrm{d}t.$$

The formulation has the same flavour as the Case II.

Here, $\dot{l}_i$ is calculated as

$$\begin{aligned} l_i^2(t) &= (\boldsymbol{R} p_i(0) - q_i)^T (\boldsymbol{R} p_i(0) - q_i) \\ &= p_i^T(0) p_i(0) + q_i q_i^T - 2 p_i^T(0) \boldsymbol{R}^T q_i \\ 2 l_i \dot{l}_i(t) &= -2 p_i(0) \dot{\boldsymbol{R}}^T(t) q \\ \dot{l}_i(t) &= -p_i(0) \dot{\boldsymbol{R}}^T(t) q / l_i, \end{aligned}$$

and $\dot{\boldsymbol{R}}^T$ can be obtained using

$$\dot{\boldsymbol{R}} = \dot{\theta} \frac{\partial \boldsymbol{R}}{\partial \theta} + \dot{\phi} \frac{\partial \boldsymbol{R}}{\partial \phi}$$

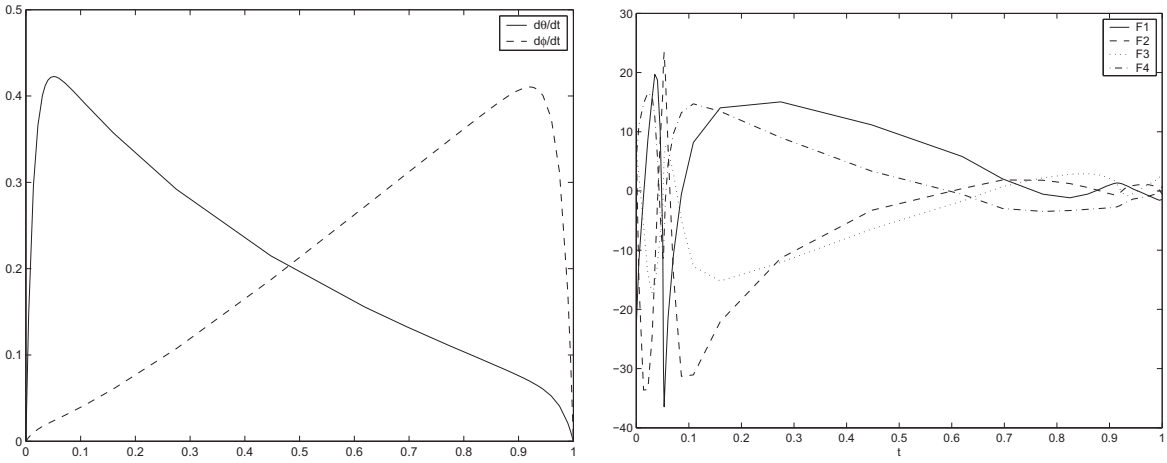

(a) $\dot{\theta}, \dot{\phi}$

(b) Muscle force variations for the optimal path

Figure 7.5: $\dot{\theta}, \dot{\phi}$ and four rectus muscle forces corresponding to Optimal path from $(\pi/6, \pi/6)$ to $(\pi/10, \pi/10)$ for Case II

Figure 7.7 shows the optimal path. Parameters for oblique muscles were chosen such that they have a very small activity. Figures 7.8, 7.9 show only the corresponding rectus muscle activities.

7.3 Comparison of Lengths of Eye Rotations

Here we present numerical results to compare lengths of minimal eye rotations with and without the Listing constraint. The length $\ell(\sigma)$ of the curve $\sigma(t)$ is given by integrating the magnitude of the tangent vector $\sigma'(t)$ in t as

$$\begin{aligned}
\ell(\sigma) &= \int_a^b \left\| \dot{\theta}\frac{\partial}{\partial\theta} + \dot{\phi}\frac{\partial}{\partial\phi} \right\| \, \mathrm{d}t \\
&= \int_a^b \sqrt{\dot{\theta}^2 g_{11} + 2\dot{\theta}\dot{\phi} g_{12} + \dot{\phi}^2 g_{22}} \, \mathrm{d}t \\
&= \int_a^b \sqrt{4\sin^2(\phi/2)\dot{\theta}^2 + \dot{\phi}^2} \, \mathrm{d}t.
\end{aligned}$$

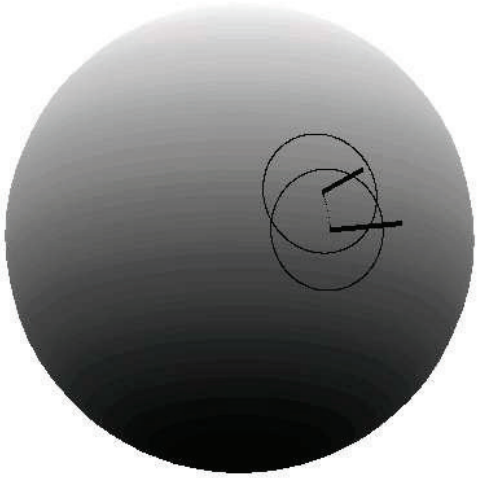

Figure 7.6: Optimal path in R^3 for Case II

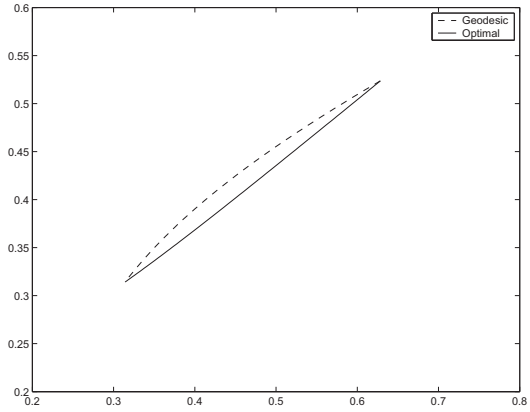

Figure 7.7: Optimal path from $(\pi/5, \pi/6)$ to $(\pi/10, \pi/10)$

In the case when the Listing's law is observed, we compute the geodesic distances as well as distances along curves that minimize the energy function considered in the section 7.2.1 (see Table 7.1).

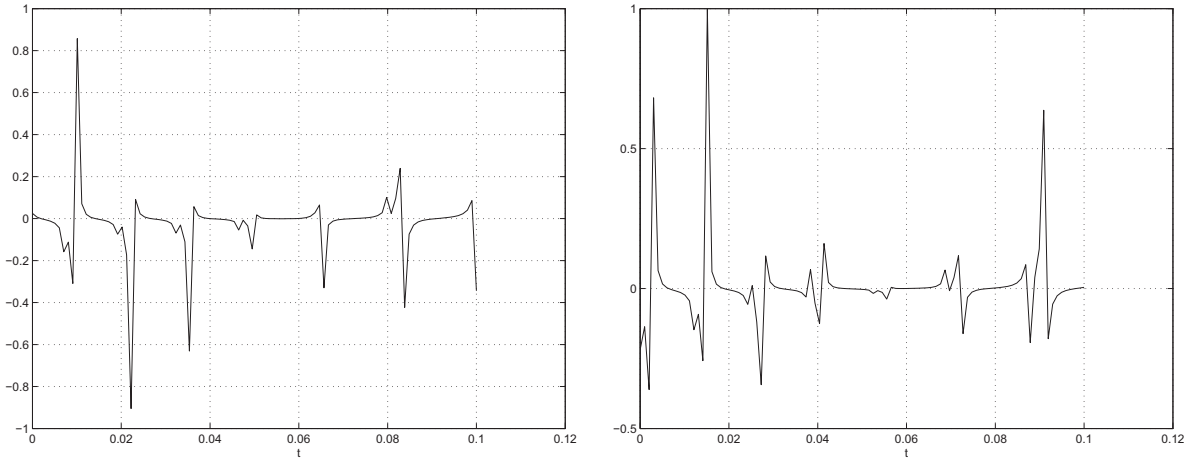

(a) Lateral rectus muscle activity (b) Medial rectus muscle activity

Figure 7.8: Lateral and medial rectus muscle activities for Case III

Table 7.1: Comparison of Lengths of Eye Rotations

From	**To**	**distance** (radians)		
(θ, ϕ)	(θ, ϕ)	$SO(3)$	**Geodesic on List**	**Min. energy on List**
$(\frac{\pi}{4}, \frac{\pi}{6})$	$(\frac{\pi}{8}, \frac{\pi}{8})$	0.219	0.222	0.324
$(\frac{\pi}{4}, \frac{\pi}{4})$	$(\frac{\pi}{8}, \frac{\pi}{6})$	0.359	0.368	0.368
$(\frac{\pi}{6}, \frac{\pi}{10})$	$(\frac{\pi}{8}, \frac{\pi}{4})$	0.476	0.480	0.482

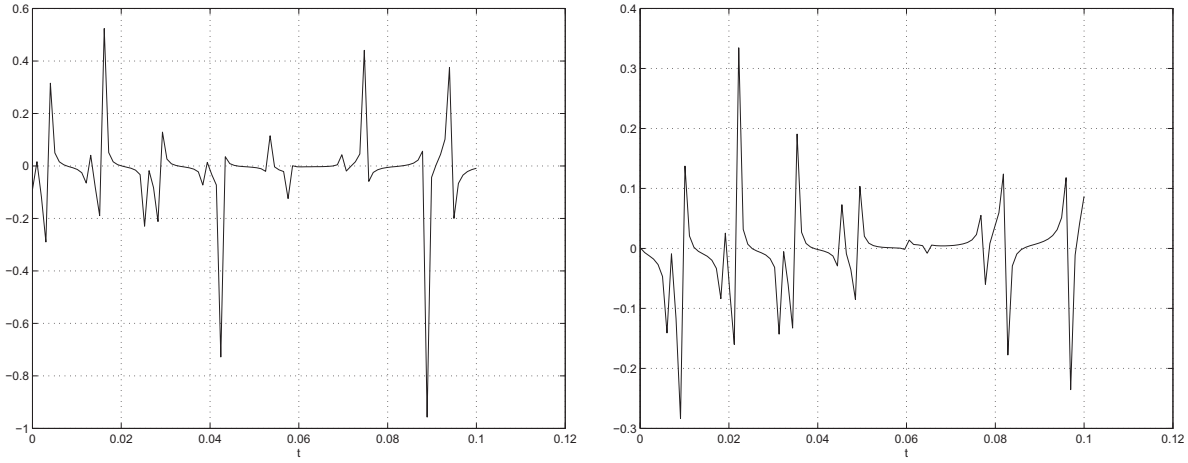

(a) Superior rectus muscle activity

(b) Inferior rectus muscle activity

Figure 7.9: Superior and inferior rectus muscle activities for Case III

Chapter 8

Conclusions

The best material model of a cat is another, or preferably the same, cat.

— Norbert Wiener

8.1 Summary

Though the planer eye movement problem has been thoroughly looked at in a modeling point of view first by Robinson (see [Robinson 1964]) and then by many others (see [Miller & Robinson 1984, Martin & Schovanec 1998]), there has not been a successful attempt to model the three-dimensional eye movements. This is partly because of the clouded interpretations (misunderstandings, rather) of *Listing's law* and the lack of a geometric setting to describe it.

In this dissertation, we have described, in detail, the Riemannian geometry of the Listing space. An interesting, yet simple local coordinate system is proposed and the corresponding Riemannian metric is derived. This setting enables one to clearly state the Listing's law in a geometric language.

There have been several notable studies on the geometry of eye rotations in the past (see e.g. [Handzel & Flash 1996], [Haslwanter 1995], [Hepp 1990] and [Opstal 1988]). In particular, [Handzel & Flash 1996] describes this geometry using Lie theory, as the quotient space $\mathsf{SO}(3)/\mathsf{SO}(2)$. However, Listing space, being a submanifold of $\mathsf{SO}(3)$, cannot be naturally identified as this quotient space. Furthermore, as we point out in section 6.1, Listing space is diffeomorphic to the *real projective space*, whereas $\mathsf{SO}(3)/\mathsf{SO}(2)$ is diffeomorphic to S^2. As far as

we are aware, our study is the first to explicitly describe the Riemannian geometry of the submanifold (we call it ***List***) of Listing rotations.

Once the geometry of ***List*** is clearly understood, we propose and formulate how the eye movement system can be studied as a simple mechanical control system ([Smale 1970*a*, Smale 1970*b*]). This is described in Chapter 7. This enables one to use various neuro-muscular models to make it more realistic as described in Chapter 7. Different control schemes are studied with the eye movement, to best understand the strategy used by the brain in motor control.

The purpose of such a model is three-folds. One is purely as an academic exercise. Thorough understanding of human movements is a pathway to better understand the role of brain in planning, controlling and executing different tasks. Second, as a clinical utility and scientific validity. As a clinical tool, it can help assimilate patient data, aiding diagnoses, and clarifying treatment possibilities. As a scientific hypothesis, such a model can explain many disorders in eye movements. The third, one could say, in the ever growing area of robotics.

8.2 Future directions

- The fast eye movements known as saccades (see Section 2.2 and Chapter 5) last for about 40ms. Thus a better approach in the saccadic eye movement control, would be to minimize the time instead of the control input. Time-optimal control problem could become rather difficult with the higher dimensionality in control. With six muscles contributing to the movement, dimension becomes six. The time-optimal problem with only the generalized torques τ_θ and τ_ϕ as the input, would be a good starting point.

  In this case, PMP in Section 4.4, will have the following

  $$L(x, u) \equiv 1,$$

  and

  $$\mathcal{H}(x, \lambda, u) = \langle \lambda, f(x) + u_1 g_1(x) + u_2 g_2(x) \rangle .$$

  Then using PMP one can set

  $$H(x, p) = \min_{v \in [-K,K]^2} \mathcal{H}(x, p, v)$$

where $u : [a, b] \rightarrow [-K, K]^2$. Then one may have to define the switching functions $\phi_i(t) = \langle \lambda, g_i \rangle$, $i = 1, 2$, in order to determine where the controls may switch for a *bang-bang* type control considering the vertices of $[-K, K]^2$. This would lead to an investigation of various bang- type and *singular* trajectories.

- It would be interesting to compare the model behavior with the actual eye movement recordings of humans and monkeys (eye movements in monkeys are believed to obey the Listing's law as well). Though the recodings for planer eye movements are well published and readily available (for an example, see [Robinson 1964]), such is not the case with three-dimensional eye movements.

- The Gauss curvature (we found in Section 6.3.3) being a constant on ***List*** is indeed an interesting phenomena. This suggests for a another possible parameterization of ***List***.

- In our study, we assume that the head is fixed in its position during all the eye movements. But most of our eye movements are often coupled with the movements of the head. In the case of the VOR as we discussed in Section 2.2, eye movement compensates the head movement, when one fixates the gaze on a target and a stable image is needed on the retina. VOR problem has gain much momentum in the recent past and it would be interesting to couple the kinematics and dynamics of the head movement with eye movements. VOR as well as the smooth-pursuit eye movement (see Section 2.2) provide the setting to study the tracking problem.

Appendix A

Quaternion Operations

A.1 Unit quaternions as rotations

Theorem A.1.1. *For a unit quaternion* $q = \cos(\alpha/2) + \hat{\mathbf{n}}\sin(\alpha/2)$*, the map* $\mathbf{v} \to q.\mathbf{v}.q^{-1}$ *represents a* **simple rotation** *of a vector* $\mathbf{v}$ *by an angle* α *about the axis* $\hat{\mathbf{n}}$*, in Euclidean 3-space.*

Proof. The proof requires showing that $q.\mathbf{v}.q^{-1}$ is a vector in $\mathbb{R}^3$, and a length-preserving linear transformation with no reflection component.
To see that $q.\mathbf{v}.q^{-1}$ a vector:

$$\begin{aligned}\mathbf{scal}(q.\mathbf{v}.q^{-1}) &= [(q.\mathbf{v}.q^{-1}) + (q.\mathbf{v}.q^{-1})^{-1}]/2 \qquad (\text{note: } q^{-1} = q_0 - (q_1\overrightarrow{\mathbf{i}} + q_2\overrightarrow{\mathbf{j}} + q_3\overrightarrow{\mathbf{k}}))\\ &= [q.\mathbf{v}.q^{-1} + q.v^{-1}.q^{-1}]/2\\ &= q.\mathbf{scal}(v).q^{-1} = 0.\end{aligned}$$

To see that $q.\mathbf{v}.q^{-1}$ is length preserving:

$$\begin{aligned}|q.\mathbf{v}.q^{-1}| &= |q||\mathbf{v}||q^{-1}|\\ &= |q||\mathbf{v}||q| = |\mathbf{v}|.\end{aligned}$$

To see that $q.\mathbf{v}.q^{-1}$ is a linear transformation:

$$\begin{aligned}q.(a\mathbf{v} + b\mathbf{w}).q^{-1} &= (q.a\mathbf{v}.q^{-1}) + (q.b\mathbf{w}.q^{-1})\\ &= a(q.\mathbf{v}.q^{-1}) + b(q.\mathbf{w}.q^{-1}).\end{aligned}$$

To see that $\hat{\mathbf{n}}$ is the rotation axis, we need to show that $\hat{\mathbf{n}}$ is unchanged by the rotation.

$$\begin{aligned} q.\hat{\mathbf{n}}.q^{-1} &= (\cos(\alpha/2) + \hat{\mathbf{n}}\sin(\alpha/2)).\hat{\mathbf{n}}.(\cos(\alpha/2) - \hat{\mathbf{n}}\sin(\alpha/2)) \\ &= \cos^2(\alpha/2)\hat{\mathbf{n}} - \sin^2(\alpha/2)\hat{\mathbf{n}}^3 \\ &= \hat{\mathbf{n}}. \qquad (\text{ since } \hat{\mathbf{n}}^2 = \hat{\mathbf{n}}.\hat{\mathbf{n}} = -1 \text{ and } \hat{\mathbf{n}}^3 = \hat{\mathbf{n}}^2.\hat{\mathbf{n}} = -\hat{\mathbf{n}}). \end{aligned}$$

Let the rotation angle between unit vector $\hat{\mathbf{v}}$ and $q.\hat{\mathbf{v}}.q^{-1}$ be ϕ. Therefore

$$\begin{aligned} \cos\phi &= \hat{\mathbf{v}} \,\mathbf{.}\, (q.\hat{\mathbf{v}}.q^{-1}) \\ &= \mathbf{scal}(\hat{\mathbf{v}}^{-1}.q.\hat{\mathbf{v}}.q^{-1}) \quad (\text{note, for a pure quaternion, i.e., a vector, } \hat{\mathbf{v}}^{-1} = -\hat{\mathbf{v}}) \\ &= \mathbf{scal}(-\hat{\mathbf{v}}.(\cos(\alpha/2) + \hat{\mathbf{n}}\sin(\alpha/2)).\hat{\mathbf{v}}.(\cos(\alpha/2) - \hat{\mathbf{n}}\sin(\alpha/2))) \\ &= \mathbf{scal}(\cos^2(\alpha/2) - \sin^2(\alpha/2) - (\hat{\mathbf{n}} + \hat{\mathbf{v}}.\hat{\mathbf{n}}.\hat{\mathbf{v}})\sin(\alpha/2)\cos(\alpha/2)) \end{aligned}$$

Now, $\hat{\mathbf{v}}.\hat{\mathbf{n}} = -\hat{\mathbf{v}} \,\mathbf{.}\, \hat{\mathbf{n}} + \hat{\mathbf{v}} \times \hat{\mathbf{n}} = \hat{\mathbf{v}} \times \hat{\mathbf{n}}$,
and $\hat{\mathbf{v}}.\hat{\mathbf{n}}.\hat{\mathbf{v}} = (\hat{\mathbf{v}}.\hat{\mathbf{n}}).\hat{\mathbf{v}} = -(\hat{\mathbf{v}} \times \hat{\mathbf{n}}) \,\mathbf{.}\, \hat{\mathbf{v}} + (\hat{\mathbf{v}} \times \hat{\mathbf{n}}) \times \hat{\mathbf{v}} = \hat{\mathbf{n}}$
Therefore,

$$\begin{aligned} \cos\phi &= \mathbf{scal}(\cos^2(\alpha/2) - \sin^2(\alpha/2) - 2\hat{\mathbf{n}}\sin(\alpha/2)\cos(\alpha/2)) \\ &= \cos^2(\alpha/2) - \sin^2(\alpha/2) \\ &= \cos\alpha \end{aligned}$$

and the rotation angle $\phi = \alpha$. □

A.2 Quaternion algorithms

A.2.1 Quaternions to rotation matrices

Let $q = q_0 + \mathbf{q}$ be a unit quaternion and $\mathbf{v}$ be a vector in $\mathbb{R}^3$. Then the rotation operator in given in Theorem A.1.1 gives a vector

$$\begin{aligned} \mathbf{w} = q.\mathbf{v}.q^{-1} &= (q_0 + \mathbf{q}).(0 + \mathbf{v}).(q_0 - \mathbf{q}) \\ &= (2q_0^2 - 1)\mathbf{v} + 2(\mathbf{q} \,\mathbf{.}\, \mathbf{v})\mathbf{q} + 2q_0(\mathbf{q} \times \mathbf{v}) \\ &= (q_0^2 - |\mathbf{q}|^2)\mathbf{v} + 2(\mathbf{q} \,\mathbf{.}\, \mathbf{v})\mathbf{q} + 2q_0(\mathbf{q} \times \mathbf{v}) \end{aligned} \tag{A.1}$$

Note that

$$(2q_0^2-1)\mathbf{v} = \begin{bmatrix} (2q_0^2-1) & 0 & \\ 0 & (2q_0^2-1) & 0 \\ 0 & 0 & (2q_0^2-1) \end{bmatrix} \begin{bmatrix} v_1 \\ v_2 \\ v_3 \end{bmatrix}$$

$$2(\mathbf{q}\,.\,\mathbf{v})\mathbf{q} = \begin{bmatrix} 2q_1^2 & 2q_1q_2 & 2q_1q_3 \\ 2q_1q_2 & 2q_2^2 & 2q_2q_3 \\ 2q_1q_3 & 2q_2q_3 & 2q_3^2 \end{bmatrix} \begin{bmatrix} v_1 \\ v_2 \\ v_3 \end{bmatrix}$$

$$2q_0(\mathbf{q}\times\mathbf{v}) = \begin{bmatrix} 0 & -2q_0q_3 & 2q_0q_2 \\ 2q_0q_3 & 0 & -2q_0q_1 \\ -2q_0q_2 & 2q_0q_1 & 0 \end{bmatrix} \begin{bmatrix} v_1 \\ v_2 \\ v_3 \end{bmatrix}$$

Therefore

$$\begin{bmatrix} w_1 \\ w_2 \\ w_3 \end{bmatrix} = \underbrace{\begin{bmatrix} 2q_0^2-1+2q_1^2 & 2q_1q_2-2q_0q_3 & 2q_1q_3+2q_0q_2 \\ 2q_1q_2+2q_0q_3 & 2q_0^2-1+2q_2^2 & 2q_2q_3-2q_0q_1 \\ 2q_1q_3-2q_0q_2 & 2q_2q_3+2q_0q_1 & 2q_0^2-1+2q_3^2 \end{bmatrix}}_{\mathbf{rot}(\mathrm{q})} \begin{bmatrix} v_1 \\ v_2 \\ v_3 \end{bmatrix} \tag{A.2}$$

with $q_0^2+q_1^2+q_2^2+q_3^2=1$.

A.2.2 Rotation matrices to quaternions

An efficient way to determine quaternion components q_1, q_2, q_3, q_4 from a matrix $M = \mathbf{rot}(\mathrm{q})$ is to use the entries M_{ij}. Upon inspection, one can write the following scheme

A.2.3 Euler angles to quaternion

Out of twelve possible axis conventions, for Euler angles, let's use the one which is popular in aeronautics, *roll*, *pitch* and *yaw*. A general rotation is obtained by first yawing around the z axis by an angle ϕ, then pitching around the y axis by θ, and finally rolling around the x axis by ψ. Therefore, the corresponding quaternions

Table A.1: Rotation matrices to quaternions conversion scheme

$q_0^2 = \frac{1}{4}(1 + M_{11} + M_{22} + M_{33})$

<table>
<tr><td colspan="4">$q_0^2 > 0$</td></tr>
<tr><td>True</td><td colspan="3">False</td></tr>
<tr><td rowspan="3">$q_0 = \sqrt{q_0^2}$
$q_1 = (M_{23} - M_{32})/4q_0$
$q_2 = (M_{31} - M_{13})/4q_0$
$q_3 = (M_{12} - M_{21})/4q_0$</td><td colspan="3">$q_0 = 0$
$q_1^2 = 1/2(M_{22} + M_{33})$</td></tr>
<tr><td colspan="3">$q_1^2 > 0$</td></tr>
<tr><td>True</td><td>False</td></tr>
<tr><td rowspan="3"></td><td rowspan="3">$q_1 = \sqrt{q_1^2}$
$q_2 = M_{12}/2q_1$
$q_3 = M_{13}/2q_1$</td><td colspan="2">$q_1 = 0$
$q_2^2 = 1/2(1 - M_{33})$</td></tr>
<tr><td colspan="2">$q_2^2 > 0$</td></tr>
<tr><td>True</td><td>False</td></tr>
<tr><td></td><td></td><td>$q_2 = \sqrt{q_2^2}$
$q_3 = M_{23}/2q_2$</td><td>$q_2 = 0$
$q_3 = 0$</td></tr>
</table>

are

$$q_{\text{roll}} = \cos(\psi/2) + \vec{\mathbf{i}} \sin(\psi/2)$$
$$q_{\text{pitch}} = \cos(\theta/2) + \vec{\mathbf{j}} \sin(\theta/2)$$
$$q_{\text{yaw}} = \cos(\phi/2) + \vec{\mathbf{k}} \sin(\phi/2).$$

Multiplying these together in the right order gives the desired quaternion $q = q_{\text{yaw}} q_{\text{pitch}} q_{\text{roll}}$, with components

$$q_0 = \cos(\psi/2)\cos(\theta/2)\cos(\phi/2) + \sin(\psi/2)\sin(\theta/2)\sin(\phi/2)$$
$$q_1 = \sin(\psi/2)\cos(\theta/2)\cos(\phi/2) - \cos(\psi/2)\sin(\theta/2)\sin(\phi/2)$$
$$q_2 = \cos(\psi/2)\sin(\theta/2)\cos(\phi/2) + \sin(\psi/2)\cos(\theta/2)\sin(\phi/2)$$
$$q_3 = \cos(\psi/2)\cos(\theta/2)\sin(\phi/2) - \sin(\psi/2)\sin(\theta/2)\cos(\phi/2)$$

Appendix B

Hill-type model of the musculotendon complex

The Hill-type model [Hill 1938, Zajac 1989] (Figure B.1) used for the musculotendon complex, has been shown to incorporate enough complexity while remaining computationally practical.

The muscle of length l_m is in series and off-axis by a pennation angle α with the tendon of length l_t. Here we assume that $\alpha = 0$. The total length of the musculotendon complex is l_{tm}. The muscle has two main components: an *active force generator* and a parallel *passive component*. The passive component consists of a parallel elastic element (F_{pe}) which describes the passive muscle elasticity and a damping component which corresponds to the passive muscle viscosity (B_m). The active component generates the active force for the muscle, which is the product

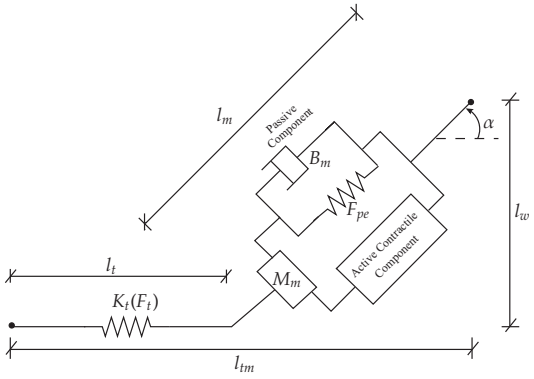

Figure B.1: Hill-type model of the musculotendon complex.

of length-tension relation $f_l(l_m)$, velocity-tension relation $f_v(\dot{l}_m)$, and the activation level $a(t)$ [Zajac 1989]. In utilizing these relationships, analytical expressions that capture the qualitative properties of the curves will be used. Alternatively, a natural cubic spline can be fitted when sufficient data is available.

In order to develop curves to describe the attributes of a generic muscle, appropriate scaling is done on the above parameters [Zajac 1989, Martin & Schovanec 1999]. The scale parameters needed for each musculotendon include: maximal isometric active muscle force, F_o, optimal muscle length, l_o, pennation angle, α_o when $l_m = l_o$, and tendon slack length l_{ts}. All forces and lengths are scaled as $\tilde{F} = F/F_o$ and $\tilde{l}_m = l_m/l_o$.

The nonlinear passive muscle force which depends on the muscle length is commonly expressed as in Equation B.1.

$$F_{pe}(l_m) = \begin{cases} (\frac{k_{ml}}{k_{me}})[exp(k_{me}(l_m - l_{ms})) - 1] & l_{ms} \leq l_m < l_{mc} \\ k_{pm}(l_m - l_{mc}) + F_{mc} & l_m > l_{mc} \\ 0 & \text{otherwise} \end{cases} \tag{B.1}$$

Here the passive muscle slack length is l_{ms} corresponds to a length at which no force is generated. The transition length from the linear to nonlinear region is l_{mc} corresponding to the force F_{mc}.

The total active force generated is quantified as the product of the force-length and force-velocity curves and the resulting surface is scaled by muscle activation. Thus the active force is formulated as

$$F_{act} = F_o f_l(\tilde{l}_m) f_v(\tilde{v}_m) \times\ a(t) \tag{B.2}$$

where $\tilde{v}_m = \dot{\tilde{l}}_m$. Figure B.2 shows the variation of muscle force with muscle length and velocity.

Muscle activation, $a(t)$, is related to the neural input $u(t)$ via the process known as contraction dynamics [Zajac 1989]. This process is known to be mediated through a calcium diffusion and is represented by a first order differential equation

$$\frac{da(t)}{dt} + \left[\frac{1}{\tau_{act}}(\beta + (1-\beta)u(t))\right] a(t) = \frac{1}{\tau_{act}} u(t) \tag{B.3}$$

where $0 < \beta < 1$ and τ_{act} is an activation time constant that varies with fast and slow muscle.

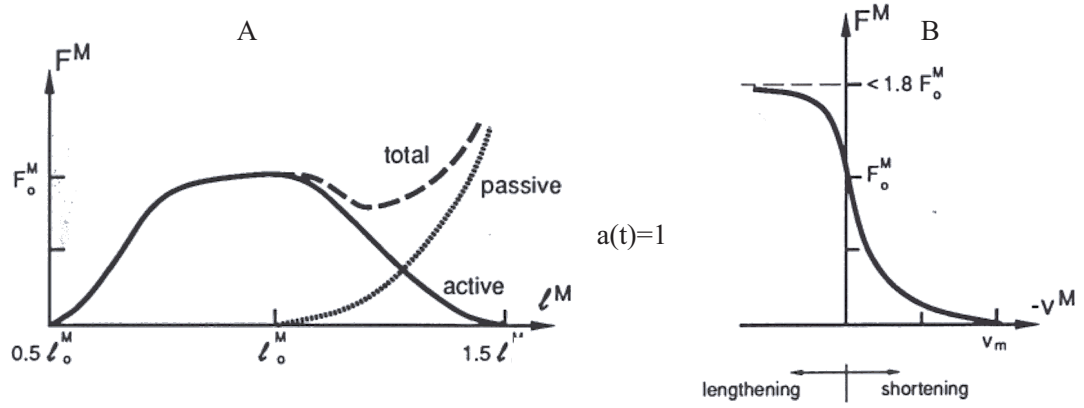

Figure B.2: **A**: Isometric Force-length relation and **B**: Force-velocity relation, for muscle with full activation, i.e., $a(t) = 1$ (Zajac, 1989)

The tendon shown in Figure B as the series elastic element, assumed to behave non-linearly under minimal extension and then to become linear with stiffness constant k_s beyond a given length l_{tc} associated with a particular level of resisting force, F_{tc}. A common approach is to assume a model of the form

$$\dot{F}_t = K_t(F_t)\dot{l}_t \tag{B.4}$$

where

$$K_t(F_t) = \begin{cases} k_{te}F_t + K_{tl}, & 0 \le F_t < F_{tc} \\ k_s, & F_t \ge F_{tc} \end{cases} \tag{B.5}$$

Equation (B.4) can be integrated to obtain F_t:

$$F_t(l_t) = \begin{cases} \frac{k_{tl}}{k_{te}}(e^{k_{te}(l_t - l_{ts})} - 1), & l_{ts} \le l_t < l_{tc} \\ k_s(l_t - l_{tc}) + F_{tc}, & l_t > l_{tc} \\ 0, & otherwise \end{cases} \tag{B.6}$$

Therefore, the total force in the muscle

$$F_t - (F_{act} + F_{pe} + B_m\dot{l}_m) \tag{B.7}$$

References

Abraham, R. & Marsden, J. E. (1987), *Foundations of Mechanics*, second edn, Addison Wesley, Reading, MA.

Agrachev, A. A. & Sachkov, Y. L. (2003), 'Control theory from the geometric viewpoint', Scuola Internazionale Superiore di Studi Avanzati (SISSA), Trieste, Italy. Lecture Notes.

Agrachev, A. A., ed. (2001), *Mathematical Control Theory*, Vol. VIII of *ICTP Lecture Notes Series*, The Abdus Salam International Centre for Theoretical Physics, Trieste, Italy.

Agrachev, A. A., Stefani, G., & Zezza, P. (n.d.), 'Strong optimality for a Bang-Bang trajectory', *SIAM J. Control Optim.* accepted.

Arnol'd, V. I. (1989), *Mathematical Methods of Classical Mechanics*, number 60 *in* 'Graduate texts in mathematics', second edn, Springer-Verlag, New York-Heidelberg-Berlin.

Athans, M. & Falb, P. L. (1966), *Optimal Control*, McGraw-Hill.

Boothby, W. M. (1986), *An Introduction to Differentiable Manifolds and Riemannian Geometry*, Academic Press, CA.

Boscain, U. & Piccoli, B. (2004), *Optimal Syntheses for Control Systems on 2-D Manifolds*, Vol. 43 of *Mathématiques et Applications*, Springer-Verlag.

Brocket, R. W. (1978), Feedback invariants for nonlinear systems, *in* 'Proceedings of the 6th IFAC Congress', Helsinki, Finland.

Brockett, R. W. (1982), Control theory and singular Riemannian geometry, *in* P. J. Hilton & G. S. Young, eds, 'New Directions in Applied Mathematics', Springer-Verlag, New York, pp. 11–27.

Bullo, F. (1999), Nonlinear Control of Mechanical Systems: A Riemannian Geometry Approach, PhD dissertation, California Institute of Technology, Pasadena, CA.

Bullo, F. & Lewis, A. D. (2004), *Geometric Control of Mechanical Systems*, Springer-Verlag. To be published.

Conway, J. H. & Smith, D. A. (2003), *On Quaternions and Octonions: Their Geometry, Arithmatic, and Symmetry*, first edn, A. K. Peters, Natick, MA.

Coombs, A. T. (2000), Time-optimal control of two simple mechanical systems with three degrees of freedom and two inputs, Master's thesis, Queen's University.

Corke, P. (1996), 'A robotics toolbox for MATLAB', *IEEE Robotics and Automation Magazine* **3**(1), 24–32.

Demer, J. L., Miller, J. M., Poukens, V., Vinters, H. V. & Glasgow, B. J. (1995), 'Evidence for fibromuscular pulleys of the recti extraocular muscles', *Invest Ophthalmol Vis Sci* **36**, 1125–1136.

Demer, J., Oh, S. & Poukens, V. (2000), 'Evidence for active control of rectus extraocular muscle pulleys', *Invest Opthalmol Vis Sci.* **41**, 1280–1290.

do Carmo, M. P. (1993), *Riemannian Geometry*, Birkhäuser, Boston.

Frankel, T. (1997), *The geometry of physics : an introduction*, first edn, Cambridge University Press.

Fuchs, A., Scudder, C. & Kaneko, C. (1988), 'Discharge patterns and recruitment order of identified motoneurons and interneuclear neurons in the monkey abducens nucleus', *J. of Neurophysiology* **60**, 1874–1895.

Goldstein, H. (1980), *Classical Mechanics*, Addison-Wesley, MA.

Gray, A. (1993), *Modern differential geometry of curves and surfaces*, first edn, CRC Press, Inc., Boca Raton, Florida.

Handzel, A. A. & Flash, T. (1996), The geometry of eye rotations and Listing's law, *in* D. S. Touretzky, M. C. Mozer & M. E. Hasselmo, eds, 'Advances in Neural Information Processing Systems', Vol. 8, The MIT Press, pp. 117–123.

Haslwanter, T. (1995), 'Mathematics of three-dimensional eye rotations', *Vision Res.* **35**, 1727–1739.

Haslwanter, T. (2000), Computational and experimental aspects of rotatory eye movements in three dimensions, Technical report, Dept of Physics, ETH, Zurich, Switzerland. Submitted for obtaining the "Habilitation".

Haslwanter, T., Straumann, D., Hepp, K., Hess, B. & Henn, V. (1991), 'Smooth pursuit eye movements obey Listing's law in the monkey', *Exp.Brain Res.* **87**, 470–472.

Hepp, K. (1990), 'On Listing's law', *Commun. Math. Phys.* **132**, 285–292.

Hill, A. (1938), 'The heat of shortening and dynamic constants of muscle', *Proc. Roy. Soc. B.* **126**, 136–195.

Isidori, A. (1997), *Nonlinear Control Systems*, third edn, Springer-Verlag, New York, NY.

Jacobson, N. (1974), *Basic Algebra I*, W.H. Freeman and Company, CA.

Jurdjevic, V. (1997), *Geometric Control Theory*, Cambridge University Press.

Kalman, R. E. (1960), 'Contributions to the theory of optimal control', *Bol. Soc. Mat. Mexicana* **5**, 102–119.

Krishnaprasad, P. S., Yang, R. & Dayawansa, W. P. (1991), Control problems on principal bundles and nonholonomic mechanics, *in* 'Proceedings of the 30th IEEE Conference on Decision and Control', Vol. 2, IEEE, pp. 1133–1138.

Kuipers, J. (1998), *Quaternions and rotation sequences*, Princeton University Press, NJ.

Lewis, A. D. (1995), Aspects of Geometric Mechanics and Control of Mechanical Systems, PhD dissertation, California Institute of Technology, Pasadena, CA.

Lewis, A. D. (1999), 'Affine connection control systems', IFAC Workshop on Lagrangian and Hamiltonian Methods for Nonlinear Control.

Lewis, A. D. & Murray, R. M. (1997), 'Configuration controllability of simple mechanical control systems', *SIAM Journal of Control and Optimization* **35**(3), 766–790.

Marsden, J. E. & Ratiu, T. S. (1999), *Introduction to Mechanics and Symmetry*, Springer-Verlag.

Martin, C. & Schovanec, L. (1998), 'Muscle mechanics and dynamics of ocular motion', *J. of Mathematical Systems, Estimation and Control* **8**, 1–15.

Martin, C. & Schovanec, L. (1999), 'The control and mechanics of human movement systems', *Progress in Systems and Control Theory* **25**, 173–202.

Miller, J. (1989), 'Functional anatomy of normal human rectus muscle', *Vision Res.* **29**, 223–240.

Miller, J. & Robinson, D. (1984), 'A model of the mechanics of binocular alignment', *Computers and Biomedical Research* **17**, 436–470.

Minor, L. B., Lasker, D. M., Backous, D. D. & Hullar, T. E. (1999), 'Horizontal vestibuloocular reflex evoked by high-acceleration rotations in the squirrel monkey. I. normal responses', *J.Neurophysiol* **82**, 1254–1270.

Misslisch, H., Tweed, D., Fetter, M., Sievering, D. & Koenig, E. (1994), 'Rotational kinematics of the human vestibuloocular reflex. III. Listing's law', *J. of Neurophysiology* **72**, 2490–2502.

Murray, R. M. (1997), 'Nonlinear control of mechanical systems: a Lagrangian perspective', *Annual Reviews in Control* **21**, 31–45.

Murray, R. M. (2004), 'Future directions in control, dynamics, and systems: Overview, grand challenges, and new courses', *European Journal of Control*. To appear.

Murray, R. M., Li, Z. & Sastry, S. S. (1994), *A mathematical introduction to robotic manipulation*, CRC Press, Inc., Boca Raton, Florida.

Nishikawa, S. (2001), *Variational Problems in Geometry*, Vol. 205 of *Translations of Mathematical Monographs*, American Mathematical Society.

Noble, J. & Schättler, H. (2002), 'Sufficient conditions for relative minima of broken extremals in optimal control theory', *J. Math. Anal. Appl.* **269**, 98–128.

Oliva, W. M. (2002), *Geometric Mechanics*, Lecture notes in mathematics, Springer Verlag.

Opstal, J. V. (1988), Three-dimensional kinematics underlying gaze control, *in* E. Domany, J. L. V. Hemman & K. Schultan, eds, 'Models of Neural Networks IV', Springer Verlag.

Optican, L. M. (1994), Control of saccadic trajectory by the superior colliculus, *in* 'Contemporary Ocular Motor and Vestibular Research: A Tribute to David A. Robinson', Stuttgart,Thieme, pp. 98–105.

Polpitiya, A. D. & Ghosh, B. K. (2002), Modelling and control of eye-movement with musculotendon dynamics, *in* 'Proceedings of the American Control Conference', Vol. 3, IEEE, pp. 2313–2318.

Polpitiya, A. D. & Ghosh, B. K. (2003), Modeling the dynamics of oculomotor system in three dimensions, *in* 'Proceedings of the 42nd IEEE Conference on Decision and Control', IEEE.

Polpitiya, A. D., Ghosh, B. K., Martin, C. F. & Dayawansa, W. P. (2004), Mechanics of the eye movement: Geometry of the Listing space, Submitted to the American Control Conference.

Polpitiya, A. D., Simpson, W. & Ghosh, B. K. (2002), Modeling and control of eye movements with musculotendon dynamics, *in* 'Proceedings of the Annual Computational Neuroscience Meeting'.

Pontryagin, L. S., Boltyanskii, V. G., Gamkrelidze, R. V. & Mishchenko, E. F. (1964), *The mathematical theory of optimal processes*, Pergmon Press, Oxford, England.

Quaia, C. & Optican, L. (1998), 'Commutative saccadic generator is sufficient to control a 3-d ocular plant with pulleys', *J. of Neurophysiology* **79**, 3197–3215.

Raphan, T. (1998), 'Modeling control of eye orientation in three dimensions. 1. role of muscle pulleys in determining saccadic trajectory', *J. of Neurophysiology* **79**, 2653–2667.

Robinson, D. (1964), 'The mechanics of human saccadic eye movement', *J. of Physiology* **174**, 245–264.

Shoemake, K. (1985), Animating rotation with quaternion curves, *in* 'ACM SIGGRAPH', Vol. 19, pp. 245–254.

Smale, S. (1970*a*), 'Topology and mechanics, I.', *Inventiones Mathematicae* **10**, 305–331.

Smale, S. (1970*b*), 'Topology and mechanics, II.', *Inventiones Mathematicae* **11**, 45–64.

Sugathadasa, M. S., Dayawansa, W. P. & Martin, C. F. (2000), Control of pursuit eye movement, *in* 'Proceedings of the 39th IEEE Conference on Decision and Control', Vol. 2, IEEE, pp. 1793–1798.

Sussman, H. J. (1998), Geometry and optimal control, *in* J. Baillieul & J. C. Willems, eds, 'Mathematical Control Theory', Springer-Verlag, New York, pp. 140–198. in honor of Roger W. Brockett on the occasion of his 60th birthday.

Sussman, H. J. & Willems, J. C. (1997), '300 years of optimal control: From the Brachystochrone to the Maximum Principle', *IEEE Control Systems Magazine*.

Sussman, H. J. & Willems, J. C. (2000), The Brachistrone problem and modern control theory, *in* A. Anzaldo-Meneses, B. Bonnard, J. P. Gauthier & F. Monroy-Perez, eds, 'Proceedings of the conference on Geometric Control Theory and Applications held in honor of Velimir Jurdjevic on the occasion of his 60th birthday', Also to appear in Contemporary trends in non-linear geometric control theory and its applications, World Scientific Publishers.

Sussmann, H. J. (1987), 'A general theorem on local controllability', *SIAM Journal of Control and Optimization* **25**(2), 158–194.

Tweed, D. & Villis, T. (1987), 'Implications of rotational kinematics for the oculomotor system in three dimensions', *J. of Neurophysiology* **58**, 832–849.

Tweed, D. & Villis, T. (1990), 'Geometric relations of eye position and velocity vectors during saccades', *Vision Res.* **30**, 111–127.

Tweed, D., Fetter, M., Andreadaki, S., Koenig, E. & Dichgans, J. (1992), 'Three-dimensional properties of human pursuit eye movements', *Vision Res.* **32**, 1225–1238.

Tweed, D., Haslwanter, T. & Fetter, M. (1998), 'Optimizing gaze control in three dimensions', *Science* **281**, 1363–1366.

van Opstal, A. J., Hepp, K., Hess, B. J., Straumann, D. & Henn, V. (1991), 'Two-rather than three-dimensional representation of saccades in monkey superior colliculus', *Science* **252**, 1313–1315.

Warner, F. W. (1989), *Foundations of Differentiable Manifolds and Lie Groups*, Vol. 94 of *Graduate Texts in Mathematics*, second edn, Springer-Verlag, NY.

Yang, R. (1992), Nonholonomic Geometry, Mechanics and Control, PhD thesis, Institute for Systems Research, University of Maryland, College Park, MD.

Yang, R., Krishnaprasad, P. S. & Dayawansa, W. P. (1996), Optimal control of a rigid body with two oscillators, *in* 'Proceedings of Mechanics Day, Fields Institute Communications', Vol. 7, Amer. Math. Soc., Providence.

Zajac, F. (1989), 'Muscle and tendon: Properties, models, scaling, and application to biomechanics and motor control', *CRC Critical Reviews in Biomedical Engineering* **17**, 359–411.

Index